JOURNAL OF GEOPHYSICAL RESEARCH, VOL. 111, B11105, doi:10.1029/2005JB003874, 2006

A geomagnetic estimate of mean paleointensity

C. V. Voorhies[1]

Received 7 June 2005; revised 28 June 2006; accepted 18 July 2006; published 22 November 2006.

[1] A statistical hypothesis about Earth's magnetic field is tested against paleomagnetism by combining it with the present field to estimate mean paleointensity. The estimate uses the satellite era geomagnetic multipole power spectrum R_n, which gives the mean square magnetic induction represented by spherical harmonics of degree n averaged over the sphere of radius a = 6371.2 km. The hypothesis asserts that low-degree multipole powers of the core source field, R_n^c, are distributed as chi-square with $2n + 1$ degrees of freedom and theoretical expectation values $\{R_n^c\} = K(n + 1/2)[n(n + 1)]^{-1}(c/a)^{2n+4}$, where c is the 3480 km radius of Earth's core. The implied field is usually mainly dipolar and can be primarily axial. Amplitude K is estimated by fitting theoretical to observational spectra of degrees 1–12. The resulting calibrated expectation spectrum is summed through degree 12 to estimate expected square intensity $\{F^2\}$. This sum also estimates mean square paleointensity, averaged over geologic time as well as the sphere, in so far as the present field spectrum is a fair sample of that generated in the past by core geodynamic processes. Previously, we excluded dominant degrees 1 and 2 from the fit, but not the sum, to "predict" mean paleointensity from the 1980 Magsat nondipole field. The new estimate fits all R_n of degrees 1–12 self-consistently and yields $\{F^2\} = (37.3 \pm 4.3\ \mu\mathrm{T})^2$. Expected paleointensity $\{F\}$ is about 34.4 ± 4.9 μT; expected virtual axial dipole moment is about $(6.51 \pm 0.94) \times 10^{22}$ Am^2. These estimates are within the range of published paleomagnetic determinations of mean paleointensity; therefore the statistical hypothesis passes this test.

Citation: Voorhies, C. V. (2006), A geomagnetic estimate of mean paleointensity, *J. Geophys. Res.*, *111*, B11105, doi:10.1029/2005JB003874.

1. Introduction

[2] The present geomagnetic field is but a sample of a field which has existed for much of geologic time, yet the question of whether or not the present field is typical of the past has been largely answered by paleomagnetism [see, e.g., *Merrill and McElhinny*, 1983; *Jacobs*, 1994]. The present field on Earth's surface is predominantly that of a roughly axial geocentric dipole. Paleodirection data show that the past field has also been predominantly that of a roughly axial dipole, except during infrequent, geologically brief, dipole excursions and reversals. Furthermore, paleointensity data indicate that the mean magnetic intensity on Earth's surface, when averaged over many millions of years, is within a factor of two of its present mean value. It follows that some statistical hypotheses about Earth's magnetic field can be tested using both direct geomagnetic measurements and inferential paleomagnetic data.

[3] To test one such hypothesis, *Voorhies and Conrad* [1996] used the nondipole main field at Magsat epoch 1980 to "predict" mean paleointensity and mean virtual axial dipole moment. The resulting values, about 32.8 μT and 6.21×10^{22} Am^2 respectively, were within the ranges found in published paleointensity studies – albeit perhaps less than most. So the hypothesis passed a test and a key to past behavior of Earth's dipole field was found in the modern nondipole field.

[4] Now, however, the physical hypotheses of narrow-scale flow and a dynamically weak magnetic field by the top of the core, as developed and tested in paper 1 [*Voorhies*, 2004], require a modification of our original statistical hypothesis. Moreover, a fully self-consistent calibration of the statistical model against the satellite era main field is possible and the result can be used to estimate common measures of mean paleointensity without any of the additional assumptions previously thought necessary. There are also more paleomagnetic determinations of mean paleointensity with which to test the statistical hypothesis.

[5] To better test both physical and statistical hypotheses, and to demonstrate the utility of paleomagnetic determinations of mean paleointensity, let us develop the model in sections 2 and 3; estimate mean paleointensity, mean virtual moments and uncertainties in sections 4 and 5; and compare such geomagnetic estimates with published paleomagnetic determinations in section 6.

[6] A review of statistical magnetic field models is outside the scope of this article [*Constable and Parker*, 1988; *Hulot and LeMouël*, 1994; *Constable et al.*, 1998; *Love and Constable*, 2003]. It is stressed that the model considered here is incomplete: it does not specify probability densities (PDs) for all the Gauss coefficients; it merely assigns trial PDs to specific nonlinear combinations of coefficients describing a core source field. This incomplete

[1]Planetary Geodynamics, NASA Goddard Space Flight Center, Greenbelt, Maryland, USA.

statistical model is also stationary in that temporal change of PDs is not developed analytically. Fortunately, one can see what some such changes would imply for some field properties, and which physical changes in Earth's core might bring these about. The model is also compatible with a field that is usually mainly that of a geocentric axial dipole which can reverse. Indeed, it is the expectation of a largely dipolar field that enables estimation of expected paleointensity. Yet the dipole is not treated as a special exception among core source multipole moments. There is no need to.

2. Background Theory

[7] As in paper 1, denote by $\mathbf{B}(\mathbf{r}, t)$ the solenoidal magnetic induction at time t and position $\mathbf{r}$ caused by sources within the planet. Above Earth's surface, this is the potential field: $\mathbf{B} = -\nabla V$. In geocentric spherical polar coordinates (r, θ, φ), internal scalar potential V has a Schmidt-normalized spherical harmonic expansion with Gauss coefficients of degree n and order m, denoted $[g_n^m(t), h_n^m(t)]$ on a reference sphere of radius a = 6371.2 km. Coefficients through finite degree N_F can be determined by analysis of the measured field [see, e.g., *Langel*, 1987].

[8] The mean square field represented by harmonics of degree n, averaged over a sphere of radius r containing the sources, is given by the well-known Lowes-Mauersberger function

$$R_n(r,t) = (n+1)(a/r)^{2n+4}\sum_{m=0}^{n}\left[g_n^m(t)\right]^2+\left[h_n^m(t)\right]^2. \quad (1)$$

The mean square field on such a sphere is the sum from degree one to infinity of the R_n. Collectively, the R_n form a magnetic spectrum; individually, each R_n represents a multipole power. Evidently, this spectrum is dominated by a core source field at degrees less than 13 and a crustal-source field at degrees greater than 15 [see, e.g., *Langel and Estes*, 1982; *Voorhies et al.*, 2002; *Voorhies*, 2004]. The focus here is on low-degree, mainly core source, multipole powers, so instantaneous mean square surface magnetic intensity is approximated by

$$F^2(a,t) = \sum_{n=1}^{12} R_n(a,t). \quad (2)$$

This omits small corrections for ellipsoidality and topography as well as higher-degree fields.

[9] Let R_n^c denote the spectrum of the core source field alone. An expectation spectrum for the low-degree core source field, denoted $\{R_n^c\}$, is obtained in paper 1 from the hypotheses of narrow-scale flow and a dynamically weak field by the top of the core. Indeed, the same spectrum is obtained in two different ways: one an empirical approach and the other a scale-variant extension of the analysis by *Benton* [1992]. The result is written

$$\left\{R_n^c(a; n \le N_E)\right\} = K\left(n+{}^1\!/\!_2\right)[n(n+1)]^{-1}(c/a)^{2n+4}, \quad (3a)$$

where K is a constant amplitude and c denotes core radius. Spectrum (3a) is only expected to hold in a magnetic energy range of degrees no more than N_E; evidently, $N_E \ge 12$. Because very low degree multipole powers are the main contributors to mean square intensity on Earth's surface, quantitative differences between expectation spectrum (3a), our approximate spectrum

$$\left\{R_n^c(a; n \le N_E)\right\} \cong K_1[n(n+1)]^{-1/2}(c/a)^{2n+4}, \quad (3b)$$

McLeod's [1985, 1996] rule

$$\left\{R_n^c(a; n \le N_E)\right\} \cong K_M\left(n+{}^1\!/\!_2\right)^{-1}(c/a)^{2n+4}, \quad (3c)$$

and *Stevenson*'s [1983] relation

$$\left\{R_n^c(a; n \le N_E)\right\} \approx K_S n^{-1}(c/a)^{2n+4}, \quad (3d)$$

at very low degree are of interest here.

[10] Theoretical spectral variance $\{(R_n^c - \{R_n^c\})^2\}$ was not specified in paper 1; therefore tests of spectrum (3a) were limited to comparisons between magnetic estimates of c and the independent seismologic estimate c_s = 3480 km. The former agree with the latter to within the scaled uncertainties, and were coestimated with amplitude K by fitting the logarithm of theoretical spectrum (3a) to log observational spectra.

[11] Such magnetospectral estimates of c and its uncertainty arguably depend on the distribution of residuals being approximately lognormal. The residuals include contributions from (1) small errors in observational spectra determined via harmonic analyses of massive surface and satellite data sets, (2) noncore sources, (3) errors in expectation spectrum (3a), and (4) the natural variability, or scatter, about the expected spectrum arising from core geodynamic processes. The latter is thought to dominate the residuals, but the process variance one expects depends on trial probability distributions for the R_n^c rather than the true distributions of multipole powers over geologic time, which remain unknown.

[12] So let us advance trial PDs by statistical hypothesis, set c equal to c_s, and use observational spectra to better estimate spectral amplitude K alone, hence $\{R_n^c\}$. The sum of estimated $\{R_n^c\}$ is an estimate of expected mean square intensity $\{F^2\}$. Trial PDs describe trial distributions of multipole powers in time, so the sum also amounts to a geomagnetic estimate of mean square paleointensity $\langle F^2\rangle$, averaged over the reference sphere and geologic time intervals of perhaps $10^{7\pm1}$ years. If the estimate of $\{F^2\}$ differs significantly from the value of $\langle F^2\rangle$ determined by the surface-time average of paleointensity data, then the statistical hypothesis can be rejected.

3. Trial Distribution Functions

[13] The trial probability densities advanced for $R_n^c(a; n \le N_E)$, specifically for the low-degree normalized core source multipole powers $(2n+1)R_n^c/\{R_n^c\}$, are those for chi-square with $2n + 1$ degrees of freedom,

$$P_{2n+1}\left([2n+1]R_n^c/\{R_n^c\}\right) = \frac{\left[(2n+1)R_n^c/\{R_n^c\}\right]^{n-1/2}}{2^{n+1/2}\Gamma\left(n+{}^1\!/\!_2\right)} \exp\left[-(2n+1)R_n^c/2\{R_n^c\}\right], \quad (4a)$$

Table 1. Amplitude (10^{10} nT^2) and Core Radius c From Log Fits of Spectra (3b), (3c), and (3d) to Degrees 3–12 of Observational Spectra at 1980

	GSFC 12/83		M102189	
Spectrum	Amplitude	c, km	Amplitude	c, km
(3b) K_1	5.1402	3493.3	5.3041	3486.0
(3c) K_M	5.1992	3491.8	5.3649	3484.5
(3d) K_S	4.3291	3511.4	4.4671	3504.1

where Γ denotes the gamma function and $\{R_n^c\}$ is given by spectrum (3a). With definitions $\chi^2 \equiv (2n+1)R_n^c/\{R_n^c\}$ and $k \equiv 2n+1$, this can be rewritten as

$$P_{2n+1}(\chi^2) = \left[2^{n+1/2}\Gamma(n+{}^1\!/\!_2)\right]^{-1}\left[\chi^2\right]^{n-1/2}\exp\left[-\chi^2/2\right] \quad (4b)$$

$$P_k(\chi^2)\mathrm{d}\chi^2 = \left[2^{k/2}\Gamma(k/2)\right]^{-1}\left[\chi^2\right]^{(k-2)/2}\exp\left[-\chi^2/2\right]\mathrm{d}\chi^2. \quad (4c)$$

This is the familiar distribution for chi-square with k degrees of freedom [e.g., *Beyer*, 1978].

[14] Probability densities (4a) were advanced by *Voorhies and Conrad* [1996], albeit with approximate expectation spectrum (3b). Indeed, with an unmodulated expectation spectrum equal to n times spectrum (3d), and for $n > 1$, they almost follow from the model of *Constable and Parker* [1988]. As shown in Appendix A, however, PDs (4a) neither require nor prohibit a zero mean Gaussian distribution for each Gauss coefficient. We do not need to assume distributions for individual coefficients here. Because PDs (4a) neither require nor prohibit equal partitioning of multipole power among the $n + 1$ orders m within each degree n, they neither require nor prohibit magnetic isotropy and so may describe both dipole and nondipole powers.

[15] Trial PDs (4a) are completely determined by $\{R_n^c\}$, hence by the single parameter K in spectrum (3a). As a result, the expectation value $\{R_n^c\}$ (or $\{\chi^2\} = k$), variance $2\{R_n^c\}^2/(2n+1)$ (or $\{[\chi^2 - \{\chi^2\}]^2\} = 2k$), skew, kurtosis, higher moments, and most likely value $(2n-1)\{R_n^c\}/(2n+1)$ (or $\chi^2_{\max} = k - 2$) of each and every R_n^c in the magnetic energy range are all specified by amplitude K. Such efficient closure allows estimates of spectral variance, as well as the mean, to be obtained via a one parameter fit of spectrum (3a) to a fair sample of observational R_n.

[16] *McLeod*'s [1996] value for what is here denoted $K_M(c/a)^4$ in spectrum (3c) puts K_M at about 5.6×10^{10} nT^2. Subsequently, *Voorhies and Conrad* [1996] verified the utility of spectra (3b), (3c) and (3d) by fitting log observational R_n from degrees 3 though 12 of the Magsat epoch field models GSFC 12/83 [*Langel and Estes*, 1985] and M102189 [*Cain et al.*, 1990]. The coestimated amplitudes and core radii are shown in Table 1; the values for c are within 0.9% of c_s. So we set c to c_s to better estimate K_1, K_M, and K_S. The results are listed in Table 2 below new values for K based on spectrum (3a). Taking K_1 to be 5.5266×10^{10} nT^2, we summed approximate spectrum (3b) from degrees 1–12 to "predict" an expected square intensity $\{F^2\}$ of $(35.6\ \mu\mathrm{T})^2$. This sum includes the contributions from degrees 1 and 2 predicted from the fit of spectrum (3b) to degrees 3–12 of the 1980 Magsat field alone.

[17] For each value of K, K_1 or K_M in Table 2, the range of values within ±1 standard deviation is encompassed by a factor of about $(1.295)^{\pm 1}$. The ±1 standard error range factor is $(1.085)^{\pm 1}$, so Table 2 is summarized as $K \cong 5.5 \times 10^{10}$ nT$^2 \cong K_1 \cong K_M$ with a likely error of ±9%. In so far as the standard deviation provides a sample of the root of the core process variance, values for K, hence $\{F^2\}$, obtained by a similar analysis at a different geologic time could easily differ by ±1 standard deviation, or about ±30%; therefore $\{F^2\}$ can be put at roughly $(35.6 \pm 4.9\ \mu\mathrm{T})^2$.

[18] If dipole power R_1 and quadrupole power R_2 are included in the fit as well as the sum, then the estimates of K change by an insignificant 5%, to about 5.2×10^{10} nT^2 with a ±1 standard deviation range factor of $(1.537)^{\pm 1}$. The increased uncertainty comes from the strong but declining dipole and the weak but rebounding quadrupole. *Voorhies et al.* [2002] coestimate K, c, and two parameters describing a crustal source field from model CM3 of *Sabaka et al.* [2002]. The results, a smaller value for K ($(4.49 \pm 0.87) \times 10^{10}$ nT^2) and a larger value for c (3512.5 ± 63.6 km), reflect the trade-off between these parameters as well as use of R_1 and R_2.

[19] The foregoing amplitude estimates all rely on fits of log theoretical to log observational spectra, in effect using approximately lognormal instead of chi-square distributions for residuals. Near its mean, a chi-square distribution is more closely approximated by a lognormal than by a Gaussian distribution (see Appendix B). Nonetheless, a better calibration of spectrum (3a), hence PDs (4a), is attempted by estimating amplitude K in a self-consistent way.

4. A Self-Consistent Amplitude Estimate

[20] The maximum likelihood estimate of K from a set of observational R_n, regarded as R_n^c for degrees $n_{\min}$ to $n_{\max}$, maximizes the joint density function from PDs (4b) at the observations,

$$P(\text{joint}) = \prod_{n=n_{\min}}^{n_{\max}} P_{2n+1}(\chi^2) = \max. \quad (5a)$$

This quantity is maximal when its logarithm is, or when

$$\sum_{n=n_{\min}}^{n_{\max}} (n - {}^1\!/\!_2)\ln\left[(2n+1)R_n/\{R_n^c\}\right] - (n + {}^1\!/\!_2)R_n/\{R_n^c\} = \max. \quad (5b)$$

The derivative of this sum Σ with respect to K is zero. With $\{R_n^c\}$ from spectrum (3a), $d\Sigma/dK$ equal to

Table 2. Amplitude (10^{10} nT^2) From Log Fits of Spectra (3a), (3b), (3c), and (3d) to Degrees 3–12 of Observational Spectra at Magsat Epoch 1980

Spectrum	Amplitude	GSFC 12/83	M102189
(3a)	K	5.5091	5.4640
(3b)	K_1	5.5266	5.4814
(3c)	K_M	5.5443	5.4989
(3d)	K_S	5.1256	5.0939

Table 3. Amplitude (10^{10} nT^2) of Spectrum (3a) From Observational Spectra at Magsat Epoch 1980 via Estimators (7b) (K^A) and (6) (K^B)

Field Model	Degrees	K^A	K^B
GSFC 12/83	3–12	5.6677	5.7392
GSFC 12/83	1–12	5.6605	5.6838
M102189	3–12	5.6218	5.6656
M102189	1–12	5.6220	5.6122
CM3	3–12	5.6188	5.6580
CM3	1–12	5.6195	5.6048

$(d\Sigma/d\{R_n^c\})(d\{R_n^c\}/dK)$, and $d\{R_n^c\}/dK$ equal to $\{R_n^c\}/K$, the differentiation yields

$$\sum_{n=n_{\min}}^{n_{\max}} \left(K^{\mathrm{ML}}\right)^{-1}\left[\left(n+{}^1\!/\!_2\right)R_n/\{R_n^c\}-\left(n-{}^1\!/\!_2\right)\right]=0. \quad (5c)$$

This is solved for the maximum likelihood estimate of K,

$$K^{\mathrm{ML}}=\sum_{n=n_{\min}}^{n_{\max}} n(n+1)(a/c)^{2n+4}R_n(a)\times\left[\sum_{n=n_{\min}}^{n_{\max}}\left(n-{}^1\!/\!_2\right)\right]^{-1}. \quad (5d)$$

[21] Substitution of the most probable values for R_n^c, which are $(n - 1/2)\{R_n^c\}/(n + {}^1\!/\!_2)$, into (5d) verifies that it returns the maximum likelihood estimate. Substitution of the mean values $\{R_n^c\}$ into (5d) shows that it also gives a biased estimate. This is because, unlike a Gaussian, a chi-square distribution peaks at a value less than its mean. Specifically, $\{K^{\mathrm{ML}}\}$ exceeds K because each multipole power is, on average, expected to exceed its most probable value. To remove this bias from estimator (5d), scale each observational $R_n(a)$ by $(n - 1/2)/(n + 1/2)$. This yields

$$K^B=\sum_{n=n_{\min}}^{n_{\max}} n(n+1)[(n-1/2)/(n+1/2)](a/c)^{2n+4}R_n(a)\times\left[\sum_{n=n_{\min}}^{n_{\max}}(n-1/2)\right]^{-1}, \quad (6)$$

which returns the correct value K when the data amount to mean values: $\{K^B\} = K$. The scaling eliminates an expected bias of 16.7% and so is judged worthwhile.

[22] If only one multipole power were available, current best estimator (6) would reduce to

$$K(n)=\left[n(n+1)/\left(n+{}^1\!/\!_2\right)\right](a/c)^{2n+4}R_n(a). \quad (7a)$$

A simple alternative to estimator (6) is the arithmetic mean of such $K(n)$,

$$K^A=(n_{\max}-n_{\min}+1)^{-1}\cdot\sum_{n=n_{\min}}^{n_{\max}}[n(n+1)/(n+1/2)](a/c)^{2n+4}R_n(a). \quad (7b)$$

This also correctly returns K when the data amount to mean values. The standard deviation and standard error of K^A are given by the normal formulas. For K^B, which amounts to a weighted mean of the $K(n)$ with weights equal to $(n - 1/2)$, our unbiased variance estimate σ^2 is the adjusted normalized sum of square weighted residuals: $\Sigma_n[(n - 1/2)(K(n) - K^B)]^2/\Sigma_n(n - {}^1\!/\!_2)^2$ multiplied by $(n_{\max} - n_{\min} + 1)/(n_{\max} - n_{\min})$. The standard error in K^B is put at $[\sigma^2/(n_{\max} - n_{\min} + 1)]^{1/2}$.

[23] The factor $[n(n + 1)/(n + {}^1\!/\!_2)]\ (a/c)^{2n+4}$ in estimators (6) and (7b) implies that they rely far more heavily upon multipole powers of higher degree than of lower degree. This may help explain why omission of R_1 and R_2 from past log spectral fits can give more satisfactory results. Moreover, for probability densities (4a), the process standard deviation of $R_n^c(t)$ divided by its mean, denoted $\sigma_n/\{R_n^c\}$, is $(n + 1/2)^{-1/2}$. The relative variability of core multipole powers is thus expected to increase as harmonic degree decreases. For example, $(n + 1/2)^{-1/2}$ increases from 28% to 82%, almost trebling, as n decreases from 12 to 1. So the chance of finding R_1^c far from its mean is much greater than for R_{12}^c, even though the latter may vacillate with shorter timescales.

[24] Estimators (6) and (7b) omit weights reflecting errors ε_n in observational R_n, errors considered small compared with fluctuations in R_n^c over geologic time. For this to be a good approximation, we require $\varepsilon_n/R_n \ll \sigma_n/R_n$. Unlike $\sigma_n/\{R_n^c\}$, however, ε_n/R_n tends to increase with n. The R_n used are within factors of 2 to 1/3 (for R_2) of $\{R_n^c\}$, so we merely require $\varepsilon_n/R_n \ll \sigma_n/\{R_n^c\} = (n + 1/2)^{-1/2}$, or $\varepsilon_n/R_n \ll 28\%$ for $n < 13$. To satisfy this condition, we use harmonic analyses of satellite data, which accurately determine R_n through degree 12 (and more, to reduce aliasing). In light of a similar condition on errors from crustal contributions to R_n, and the heavier reliance on higher-degree R_n, we again omit spectral degrees above 12.

[25] Table 3 lists estimates of K^A from equation (7b) and K^B from equation (6) calculated at Magsat epoch 1980 from field models GSFC 12/83, M102189, and CM3. With best estimator (6), inclusion of dipole and quadrupole powers changes K^B by but 1%, instead of 5% for lognormal estimates. K^A is even less sensitive. The tabulated values are, however, all at a single epoch. As discussed in paper 1, we should use time averages of observational $R_n(a,t)$.

[26] Here we select the mean main field spectrum $R_n(a)$ from model CM4 of *Sabaka et al.* [2004], averaged over the 1965.5–2001.5 interval spanning OGO, POGO, Magsat and Oersted satellite data used in the CM4 analysis. Table 4 lists K^A from estimator (7b), K^B from estimator (6), and the standard errors calculated from the mean R_n data for degrees 3–12, 1–11, and 1–12. The effect of excluding R_{12} exceeds that of excluding both R_1 and R_2. Model CM4 reveals a 41% increase in $R_{12}(a,t)$ from Magsat epoch 1980 to Oersted epoch 2000! Together with large values of R_{12} before 1972, this contributes to an estimate for K which is slightly larger than obtained for epoch 1980 alone. For this best estimate, $K = 5.7767 \times 10^{10}$ nT^2, the standard

Table 4. Amplitude (10^{10} nT^2) of Spectrum (3a) From 1965.5–2001.5 Time Average of Observational Spectrum CM4 from Estimators (7b) (K^A) and (6) (K^B) With Standard Errors

Degrees	K^A	K^B
3–12	5.7284 ± 0.4196	5.6720 ± 0.4083
1–11	5.6415 ± 0.6235	5.6434 ± 0.4512
1–12	5.7112 ± 0.5735	5.7767 ± 0.4060

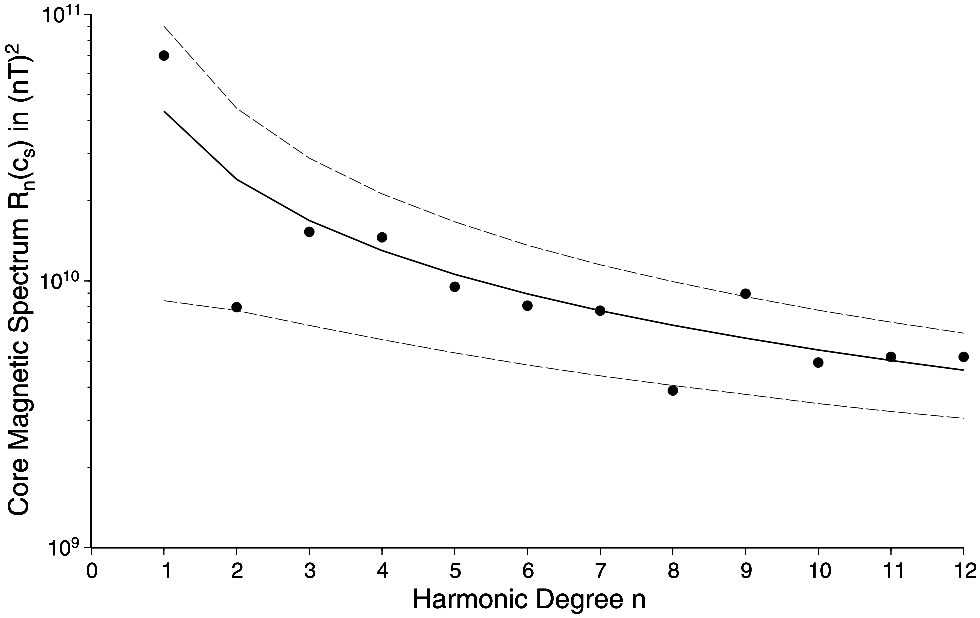

Figure 1. One parameter fit of expectation spectrum (3a) (solid curve) to satellite era averaged observational spectrum (dots) obtained with estimator (6). Spectra are multiplied by $(a/c_s)^{2n+4}$ to remove attenuation of core source field with harmonic degree n. Top and bottom dashed curves show 90% and 10% values, respectively, of the cumulative distribution functions from chi-square with $2n + 1$ degrees of freedom. Twenty percent of dots are expected to fall outside the envelope.

deviation σ is put at $\pm 1.4063 \times 10^{10}$ nT^2 and the standard error is put at $\pm 0.4060 \times 10^{10}$ nT^2.

[27] Figure 1 shows this one-parameter fit of expectation spectrum (3a) (solid curve) to the satellite era averaged main field spectrum from CM4 (dots) obtained with estimator (6); however, both theoretical and observational spectra have been multiplied $(a/c_s)^{2n+4}$ to remove the usual exponential attenuation of a core source field with harmonic degree. Also shown are the 90% and 10% values of the cumulative distribution functions from chi-square with $2n + 1$ degrees of freedom (top and bottom dashed curves, respectively). According to PDs (4a) and this fit, core multipole powers R_n^c are expected to be within the dashed curves 80% of the time. Of course, at any given point in geologic time, 20% of the multipole powers are expected to be outside this 80% envelope – two or perhaps three of the 12 points fitted. At present, dipole power is higher, and quadrupole power is lower, than expected, but both are within the range expected 80% of the geologic time. It is the degree 8 power that is lower, and the degree 9 power that is higher, than expected 80% of the time. These dominate the weighted residuals.

[28] With this best estimate for amplitude K, the sum of expectation spectrum (3a) from degrees 1–12 yields a geomagnetic estimate of expected square intensity

$$\{F^2\} = \sum_{n=1}^{12} \{R_n^c\} = (37.325 \pm 4.296\ \mu\mathrm{T})^2. \tag{8}$$

This is also the mean square paleointensity estimated by calibration of spectrum (3a) with satellite data in a manner consistent with stationary multipole power distributions (4c). The standard deviation in estimate (8) is ±24.34% of $\{F^2\}$, or ±11.51% in $\{F^2\}^{1/2}$. The estimate for $\{F^2\}^{1/2}$ is 15.17% less than the RMS intensity at 2000 (43.998 μT from CM4). The standard error indicates precision and is ±7.03% of $\{F^2\}$, or ±1.22 μT in $\{F^2\}^{1/2}$. The standard deviation is used to indicate uncertainty because the data fitted are not samples from independent times, but all depend on one realization of the core source field, a scant 36 year sample of geologic time.

5. Expected Paleointensity, VADM, and Related Quantities in a Mainly Dipolar Field

[29] With $K = 5.7767 \times 10^{10}$ nT^2 in spectrum (3a), the expected square dipole field on the reference sphere $\{R_1^c\}$ is $(33.919\ \mu\mathrm{T})^2$. This is 61.46% of R_1 at 2000 [*Sabaka et al.*, 2004], but the standard deviation of dipole power distribution (4c), σ_1, is fully 81.65% of the mean! Recent dipole power is stronger than expected from higher-degree multipoles, spectrum (3a), and PDs (4a), but only by $0.77\sigma_1$. The square nondipole field expected from degrees 2 to 12 on the reference sphere, denoted $\{R_{ND}^c\}$, is $(15.578\ \mu\mathrm{T})^2$. The ratio of expected square nondipole to dipole fields, $\{R_{ND}^c\}/\{R_1^c\}$, is 21.1%. The ratio of expected square dipole to total fields, $\{R_1^c\}/\{F^2\}$, is 82.6%. These results imply that the calibrated statistical model requires a usually mainly dipolar field on Earth's surface. This fact enables estimation of expected paleointensity and related quantities as described below.

[30] Paleointensity data are extracted from rock magnetic properties, notably thermoremanent magnetization, and thus from a part of the crustal sources. Such data are here taken as indicating the approximate surface intensity of the core source field when and where the rock last cooled, $F(a,\theta,\varphi,t_c)$. This is a fair approximation, except for data from rock magnetized (1) close to Earth's most intense crustal magnetic anomalies, (2) when an unusually weak

core source field is disturbed by very strong magnetic storms, or (3) by lightening or other subsequent alterations.

[31] An average of paleointensities from a sequence of lava flows or other igneous cooling units determines a site mean paleointensity. An average of site mean paleointensities from many different sites determines a sample mean paleointensity. Here, however, mean paleointensity is also an ideal surface-time average of F which, omitting asphericity and external fields, is

$$\langle F\rangle = [4\pi(t_f - t_i)]^{-1}\int_{t_i}^{t_f}\int_0^{2\pi}\int_0^{\pi}|\mathbf{B}(a,\theta,\varphi,t)|\sin\theta d\theta d\varphi dt, \quad (9)$$

where geologic time interval $t_f - t_i$ covers an appreciable fraction of Earth's history. An average over a denser and/or more uniform spatiotemporal sampling distribution of paleointensity data may thus yield a more accurate determination of $\langle F\rangle$.

[32] Clearly $\langle F\rangle$ is not $\langle F^2\rangle^{1/2}$; moreover, paleointensities are often reported as either virtual axial dipole moment,

$$\mathrm{VADM} \equiv \left(4\pi a^3/\mu_0\right)\left[1+3\cos^2\theta\right]^{-1/2}F(a,\theta,\varphi,t) \quad (10)$$

or virtual dipole moment,

$$\mathrm{VDM} \equiv \left(4\pi a^3/2\mu_0\right)\left[1+3\cos^2 I\right]^{1/2}F(a,\theta,\varphi,t), \quad (11)$$

where I denotes inclination [see, e.g., *Merrill and McElhinny*, 1983]. Initial efforts to test a geomagnetic value for $\{F^2\}^{1/2}$ were blocked by a lack of expressions relating $\langle\mathrm{VDM}\rangle$, $\langle\mathrm{VADM}\rangle$, and even $\langle F\rangle$, to $\langle F^2\rangle^{1/2}$. *Voorhies and Conrad* [1996] bypassed these obstacles by developing approximate expressions for $\{F\}$ and $\{\mathrm{VADM}\}$. These turn out to be good and useful approximations under more general conditions than we suspected.

[33] Formulas for expectation values of several measures of intensity are derived and evaluated below. Some exact expressions require more information than is contained in a statistical model of a core source magnetic spectrum. For example, exact calculation of expected virtual dipole moment $\{\mathrm{VDM}\}$ requires information about inclination; however, because the expected field is usually mainly dipolar, the nondipole contribution to $\{\mathrm{VDM}\}$ is fairly small and the relevant integral can be approximated in a way that eliminates any need for directional information. Because many, arguably all, viable statistical models of Earth's magnetic field will have a usually mainly dipolar field, the approximate formulas for $\{F\}$, $\{\mathrm{VADM}\}$ and $\{\mathrm{VDM}\}$ are quite widely applicable. To skip these formulas, skip to the numerical results in section 6.

5.1. Expected Absolute Dipole Moment

[34] Let $\mathbf{m}$ denote Earth's centered dipole moment. Square dipole moment $\mathbf{m}\bullet\mathbf{m}$ equals $(4\pi a^3/\mu_0)^2 R_1(a,t)/2$, so density (4a) for the degree one dipole requires $3\mathbf{m}\bullet\mathbf{m}/\{\mathbf{m}\bullet\mathbf{m}\}$ to be distributed as chi-square with three degrees of freedom. The probability of finding $|\chi|$ in the interval $[|\chi|, |\chi| + d|\chi|]$ is $P(\chi^2)[d\chi^2/d|\chi|]d|\chi|$; therefore the distribution for absolute dipole moment $|\mathbf{m}|$ implied by density (4a) is the Maxwellian distribution [see, e.g., *Reif*, 1965; *Voorhies and Conrad*, 1996]. The value for $\{R_1^c\}$ above yields a root expected square dipole moment,

$$\{\mathbf{m}\bullet\mathbf{m}\}^{1/2} = 4\pi a^3\left\{R_1^c/2\right\}^{1/2}/\mu_0, \quad (12a)$$

of 6.203×10^{22} Am^2 (ampere-turn meters^2). This is 78.4% of the 1980 value (7.907×10^{22} Am^2).

[35] For the Maxwellian, the expected absolute value is 7.9% less than the rms,

$$\begin{aligned}\{|\mathbf{m}|\} &= 4\pi a^3\left\{\left[R_1^c/2\right]^{1/2}\right\}/\mu_0 = 4\pi a^3\left[4\left\{R_1^c\right\}/3\pi\right]^{1/2}/\mu_0 \\ &= (8/3\pi)^{1/2}\{\mathbf{m}\bullet\mathbf{m}\}^{1/2},\end{aligned} \quad (12b)$$

or 5.715×10^{22} Am^2. The root of the expected process variance, $\sigma_1 = (2/3)^{1/2}\{R_1^c\}$, implies that $\pm 1\sigma_1$ variations in R_1^c would cause samples of $|\mathbf{m}|$ to range from 43% to 135% of $\{|\mathbf{m}|\}$, or from 2.45 to 7.70×10^{22} Am^2. This range is a far wider than the $\pm 11.5\%$ uncertainty in $K^{1/2}$, hence in the estimates for $\{|\mathbf{m}|\}$ and $\{\mathbf{m}\bullet\mathbf{m}\}^{1/2}$. Because the expected field is primarily dipolar, the calibrated statistical model requires a similarly wide range in paleointensities. The model does not require, but is compatible with, a dipole that is usually mainly axial, notably the hybrid Gaussian/bi-Maxwellian distribution for an axial dipole derived in Appendix A.

5.2. Expected Intensity

[36] To test a statistical model against paleomagnetic determinations of $\langle F\rangle$, we need to estimate $\{F\}$, not $\{F^2\}^{1/2}$. To do so, separate $\mathbf{B}$ into centered dipole and nondipole fields, denoted $\mathbf{B}_D$ and $\mathbf{B}_{ND}$. In dipole coordinates (θ_D, φ_D), with θ_D measured from the north pole of the tilted dipole,

$$[\mathbf{B}_D(a,\theta_D,\varphi_D,t)]^2 = \left[R_1^c(a,t)/2\right]\left(1+3\cos^2\theta_D\right). \quad (13)$$

With $\mathbf{B} = \mathbf{B}_D + \mathbf{B}_{ND}$, the expected intensity on the reference sphere is

$$\{F\} = (4\pi)^{-1}\left\{\int_0^{2\pi}\int_0^{\pi}\left[B_D^2 + 2\mathbf{B}_D\bullet\mathbf{B}_{ND} + B_{ND}^2\right]^{1/2}\sin\theta d\theta d\varphi\right\}. \quad (14a)$$

The expectation operator commutes with the surface average, so equation (14a) is rewritten as

$$\{F\} = (4\pi)^{-1}\int_0^{2\pi}\int_0^{\pi}\left\{\left[{B_D}^2 + {B_{ND}}^2\right]^{1/2} \cdot \left[1 + \frac{2\mathbf{B}_D\bullet\mathbf{B}_{ND}}{{B_D}^2 + {B_{ND}}^2}\right]^{1/2}\right\}\sin\theta d\theta d\varphi. \quad (14b)$$

[37] The expectation of a usually mainly dipolar field established above implies that the nondipole field cannot dominate integral (14b), even though PDs (4a) indicate rare intervals when $B_D^2(a,\theta,\varphi,t) \le B_{ND}^2(a,\theta,\varphi,t)$ over much of Earth's surface. So $\{F\}$ cannot differ greatly from the value

due to the dipole $\{|\mathbf{m}|\}$ alone, which is denoted $\{F_{\rm D}\}$ and is estimated to be 30.50 μT. Without fear of serious error in the integral itself, and with $\varepsilon = (2\mathbf{B}_{\rm D}\bullet\mathbf{B}_{\rm ND})/(B_{\rm D}^2 + B_{\rm ND}^2)$, the small ε approximation, $(1 + \varepsilon)^{1/2} \cong 1 + \varepsilon/2$, is used in the integrand (14b) to obtain

$$\{F\} \cong (4\pi)^{-1}\int_0^{2\pi}\int_0^{\pi}\left\{\left[B_{\rm D}^2 + B_{\rm ND}^2\right]^{1/2} \cdot\left[1+\frac{\mathbf{B}_{\rm D}\bullet\mathbf{B}_{\rm ND}}{\mathrm{B}_{\rm D}^2+\mathrm{B}_{\rm ND}{}^2}\right]\right\}\sin\theta d\theta d\varphi. \quad (14c)$$

[38] Now $\mathbf{B}_{\rm D}\bullet\mathbf{B}_{\rm ND}$ averages to zero on a sphere; moreover, densities (4a) provide no indication of correlated fluctuations between either R_1 and $R_{\rm ND}$ or $\mathbf{B}_{\rm D}$ and $\mathbf{B}_{\rm ND}$. Because $\mathbf{B}_{\rm D}\bullet\mathbf{B}_{\rm ND}$ is weighted by $[B_{\rm D}^2 + B_{\rm ND}^2]^{-1/2}$ in the integrand, its small contribution to integral (14c) need not be exactly zero. This small contribution is omitted to obtain

$$\{F\} \cong (4\pi)^{-1}\int_0^{2\pi}\int_0^{\pi}\left\{\left[B_{\rm D}^2 + B_{\rm ND}^2\right]^{1/2}\right\}\sin\theta d\theta d\varphi. \quad (15a)$$

In this integrand, the typically small term $B_{\rm ND}^2(a,\theta,\varphi,t)$ is approximated by its surface average $R_{\rm ND}^{\rm c}(a,t)$. The result is rotated into dipole coordinates $(\theta_{\rm D},\varphi_{\rm D})$; equation (13) is used to express $B_{\rm D}^2$ in terms of $R_1^{\rm c}$ and $\theta_{\rm D}$; and the integration over $\varphi_{\rm D}$ is performed to obtain

$$\{F\} \cong (1/2)\int_0^{\pi}\left\{\left[\left(R_1^{\rm c}/2\right)\left(1+3\cos^2\theta_{\rm D}\right)+R_{\rm ND}{}^{\rm c}\right]^{1/2}\right\}\sin\theta_{\rm D}d\theta_{\rm D}. \quad (15b)$$

[39] Approximation (15b) follows from PDs (4a) via the expectation of a usually mainly dipolar field alone. Three additional assumptions used by *Voorhies and Conrad* [1996] to obtain it from equation (14a) are not needed.

[40] With $x \equiv \cos\theta_{\rm D}$ and $C^2 \equiv (1 + 2R_{\rm ND}^{\rm c}/R_1^{\rm c})/3$, approximation (15b) is just

$$\{F\} \cong \left\{\left(3R_1^{\rm c}/8\right)^{1/2}\int_{-1}^{+1}\left[x^2+C^2\right]^{1/2}{\rm d}x\right\}. \quad (15c)$$

With the substitution $x = C\sinh z$ and definition $p \equiv \sinh^{-1}(1/C)$, the integral yields

$$\{F\} \cong \left\{\left(3R_1^{\rm c}/2\right)^{1/2}C^2[(\sinh 2p)/4+p/2]\right\}. \quad (15d)$$

In the limit of zero nondipole field, C^2 approaches 1/3 and approximation (15d) becomes exact.

[41] As a final approximation, replace $R_{\rm ND}^{\rm c}/R_1^{\rm c}$ with $\{R_{\rm ND}^{\rm c}\}/\{(R_1^{\rm c})^{1/2}\}^2$, so that C^2 is replaced with $C_0^2 = [1 + 2\{R_{\rm ND}^{\rm c}\}/\{(R_1^{\rm c})^{1/2}\}^2]/3$ and p with $p_0 = \sinh^{-1}(1/C_0)$. The denominator $\{(R_1^{\rm c})^{1/2}\}^2 = (8/3\pi)\{R_1^{\rm c}\}$ is chosen instead of $\{R_1^{\rm c}\}$ to help offset omission of a suspected small positive contribution to integral (14a). Then approximation (15d) simplifies to

$$\{F\} \cong \left\{\left(R_1^{\rm c}\right)^{1/2}\right\}(3/2)^{1/2}C_0^2[(\sinh 2p_0)/4+p_0/2]. \quad (15e)$$

Approximation (15e) holds for a usually mainly dipolar field.

[42] With the foregoing estimate for $\{R_1^{\rm c}\}^{1/2} = 33.919$ μT, hence $\{(R_1^{\rm c})^{1/2}\} = 31.250$ μT by equation (12b), and for $\{R_{\rm ND}^{\rm c}\}^{1/2} = 15.578$ μT, one finds $C_0^2 = 0.4990$, $p_0 = 1.1470$ and

$$\{F\} \cong 34.38 \pm 4.88\ \mu\mathrm{T}. \quad (16)$$

This value is 92.1% of the estimate for $\{F^2\}^{1/2}$, 110.0% of that for $\{(R_1^{\rm c})^{1/2}\}$, and 112.7% of that for $\{F_{\rm D}\}$. These estimates are directly proportional to $K^{1/2}$, and so have ±11.5% standard deviations. The 12.7% nondipole contribution to $\{F\}$, however, also relies on an approximation which retains terms of order $[\{R_{\rm ND}^{\rm c}\}/\{R_1^{\rm c}\}]^{1/2}$, but may omit terms of order $\{R_{\rm ND}^{\rm c}\}/\{R_1^{\rm c}\}$ or 21.1%. An error of ±12.7% × 21.1%, or ±2.7%, is thus added to the standard deviation to obtain the total uncertainty of ±14.2%, or ±4.88 μT, shown in estimate (16) for $\{F\}$.

[43] This uncertainty is much less than the square root of the core process variance from PDs (4a). Indeed, $\pm\sigma_1$ variations in $R_1^{\rm c}$ about its expected value indicate variations in dipole intensity alone from 13.1 to 41.1 μT. According to the calibrated statistical model, global mean geomagnetic intensity as a function of geologic time is expected to fluctuate about a mean of 34.4 ± 4.9 μT with a ±1 process standard deviation range somewhat wider than $\pm 1\sigma_1$, roughly 19 to 45 μT. Of course, in a primarily dipolar field that is also usually axial, a long-term average of intensity at a single geographic latitude can easily differ from this value.

5.3. Expected Virtual Axial Dipole Moment

[44] The expected virtual axial dipole moment from equation (11) is

$$\{\mathrm{VADM}\} = \left(4\pi a^3/\mu_0\right)\left\{F(a,\theta,\varphi,t_{\rm c})/\left(1+3\cos^2\theta\right)^{1/2}\right\} \quad (17a)$$

$$\{\mathrm{VADM}\} = \left(a^3/\mu_0\right)\int_0^{2\pi}\int_0^{\pi}\left\{\left[\frac{\mathrm{B}_{\rm D}^2+2\mathrm{B}_{\rm D}\bullet\mathrm{B}_{\rm ND}+\mathrm{B}_{\rm ND}^2}{1+3\cos^2\theta}\right]^{1/2}\right\} \cdot\sin\theta d\theta d\varphi. \quad (17b)$$

Expectation of a primarily dipolar field implies that the nondipole field cannot dominate this integral. A correction to $\{\mathrm{VADM}\} \approx \{|\mathbf{m}|\}$ is sought using simple approximations.

[45] As in section 5.2, the small contribution to integral (17b) from $2\mathbf{B}_{\rm D}\bullet\mathbf{B}_{\rm ND}$ is omitted and $B_{\rm ND}^2$ is approximated by $R_{\rm ND}^{\rm c}$. The result is rotated to dipole coordinates, equation (13) is used for $B_{\rm D}^2$, and the integration over $\varphi_{\rm D}$ is performed to obtain

$$\{\mathrm{VADM}\} \cong \left(4\pi \mathrm{a}^3/\mu_0\right)(1/2)\int_0^{\pi}\left\{\left[R_1^{\rm c}/2+R_{\rm ND}^{\rm c}/\left(1+3\cos^2\theta_{\rm D}\right)\right]^{1/2}\right\}\sin\theta_{\rm D}d\theta_{\rm D} \quad (18a)$$

$$\{\mathrm{VADM}\} \cong \left(4\pi a^3/\mu_0\right)\left\{\left(R_1^c/8\right)^{1/2} \cdot \int_{-1}^{+1} \left[\left(x^2+C^2\right)/\left(x^2+1/3\right)\right]^{1/2} dx\right\}. \quad (18b)$$

[46] The definite integral in approximation (18b), here denoted $I_2(C)$, is given by *Gradshteyn and Ryzhzik* [1980] in terms of elliptic integrals of the first and second kinds:

$$I_2(C) = 2C\left[F^*(\alpha,q) - E^*(\alpha,q)\right] + 2\left[3\left(C^2+1\right)/4\right]^{1/2}, \quad (19a)$$

where $\alpha = \tan^{-1}(3^{1/2}) = \pi/3 = 60°$ and $q = (C^2 - 1/3)^{1/2}/C$. Replacement of C^2 with C_0^2 as before, and q with q_0, yields

$$\{\mathrm{VADM}\} \cong \left[4\pi a^3/\mu_0\right]\left\{\left(R_1^c/8\right)^{1/2}\right\} I_2(C_0). \quad (19b)$$

Some elliptic integral tables [*Beyer*, 1978] reverse the arguments.

[47] For $C_0^2 = 0.4990$, $q_0 = 0.57619 = \sin^{-1}(35.18°)$ and $I_2 = 2.2781$; approximation (19b) yields

$$\{\mathrm{VADM}\} \cong 6.510 \times 10^{22}\ \mathrm{Am}^2. \quad (20)$$

This geomagnetic estimate of expected mean virtual axial dipole moment is 13.9% larger than that for $\{|\mathbf{m}|\}$. To allow for a 21.1% error in this correction for nondipole fields, ±2.9% is added to the ±11.5% standard deviation, to obtain an uncertainty of ±14.4%, or $\pm 0.94 \times 10^{22}$ Am^2.

[48] Analogous treatment of expected square virtual axial dipole moment leads to

$$\left\{\mathrm{VADM}^2\right\} \cong \left(4\pi a^3/\mu_0\right)^2\left\{R_1^c/2\right\}\left[1 + 3^{1/2}\left(C_0^2 - 1/3\right)(\pi/3)\right]. \quad (21a)$$

With the numerical values for C_0^2 and $\{R_1^c\}$ above, one obtains

$$\left\{\mathrm{VADM}^2\right\}^{1/2} \cong 7.07 \times 10^{22}\ \mathrm{Am}^2. \quad (21b)$$

This is 14.0% greater than $\{\mathbf{m}\bullet\mathbf{m}\}^{1/2}$. To allow for a ±21.1% inaccuracy in this correction, add ±3.0% to the ±11.5% standard deviation to obtain an uncertainty of ±14.5%, or $\pm 1.02 \times 10^{22}$ Am^2, in $\{\mathrm{VADM}^2\}^{1/2}$. Curiously, the integration over the sphere eliminates any need to assume that a primarily dipolar field is also axial to obtain these results.

5.4. Expected Virtual Dipole Moment

[49] For expected virtual dipole moment, equation (11) implies

$$\{\mathrm{VDM}\} = \left(4\pi a^3/2\mu_0\right)\left\{\left[1 + 3\cos^2 I\right]^{1/2} F(a,\theta,\varphi,t)\right\}. \quad (22a)$$

Again the expectation value implies not only integration over the sphere, but multiplying the integrand by PDs (4a) and integrating over each R_n^c. Neither the PDs nor our geomagnetic estimates of $\{R_n^c\}$ tell us what $F(a,\theta,\varphi)$ is, so these integrals could not be even approximately evaluated were it not for the fact that the statistical model requires a usually mainly dipolar field.

[50] In terms of vertical component Z, horizontal intensity H, $\tan I = Z/H$, $\cos^2 I = H^2/(Z^2 + H^2)$, and total square field $B^2 = H^2 + Z^2$, equation (22a) is equivalent to

$$\{\mathrm{VDM}\} = \left(4\pi a^3/2\mu_0\right)\left\{\left[B^2 + 3H^2\right]^{1/2}\right\}, \quad (22b)$$

or

$$\{\mathrm{VDM}\} = \left(4\pi a^3/\mu_0\right)\left\{\left[B^2 - 3Z^2/4\right]^{1/2}\right\}. \quad (22c)$$

Again we separate the field into dipole and nondipole contributions, including Z_D and Z_{ND}. With equation (13) for B_D^2, and because $Z_D^2 = 2R_1(a,t)\cos^2\theta_D$, the term $B_D^2 - 3Z_D^2/4$ is independent of $\cos\theta_D$. Equation (22c) becomes

$$\{\mathrm{VDM}\} = \left(4\pi a^3/\mu_0\right)\{[R_1/2 + 2\mathbf{B}_D\bullet\mathbf{B}_{ND} - 3Z_D Z_{ND}/2 + B_{ND}^2 - 3Z_{ND}^2/4]^{1/2}\}. \quad (22d)$$

[51] As before, expectation of a primarily dipolar field implies that the typically small nondipole contributions to the integrand can be approximated without fear of serious error in integral (22d). With $G^2 \equiv R_1/2 + B_{ND}^2 - 3Z_{ND}^2/4$, and $\varepsilon' = (2\mathbf{B}_D\bullet\mathbf{B}_{ND} - 3Z_D Z_{ND}/2)/G^2$, we use the small ε' approximation in the integrand to obtain $\{\mathrm{VDM}\} \cong (4\pi a^3/\mu_0)\{G\ [1 + \varepsilon'/2]\}$. The term $2\mathbf{B}_D\bullet\mathbf{B}_{ND} - 3Z_D Z_{ND}/2$ itself is as likely positive as negative and averages to zero on the sphere. Though weighted by about 1/2G, its small contribution to the integral is omitted, giving

$$\{\mathrm{VDM}\} \cong \left(4\pi a^3/\mu_0\right)\left\{\left[R_1/2 + B_{ND}^2 - 3Z_{ND}^2/4\right]^{1/2}\right\}. \quad (23a)$$

The mean square radial component from harmonics of degree n is $(n+1)R_n/(2n+1)$. So we further approximate B_{ND}^2 with R_{ND} and Z_{ND}^2 with $R_{ND}/2$ in equation (23a) to obtain

$$\{\mathrm{VDM}\} \cong \left(4\pi a^3/\mu_0\right)\left\{[R_1/2 + 5R_{ND}/8]^{1/2}\right\}. \quad (23b)$$

[52] One way to proceed from approximation (23b) extracts the main dipole,

$$\{\mathrm{VDM}\} \cong \left(4\pi a^3/\mu_0\right)\left\{(R_1/2)^{1/2}(1 + 5R_{ND}/4R_1)^{1/2}\right\}, \quad (24a)$$

and approximates the correction term $5R_{ND}/4R_1$ with $5\{R_{ND}\}/4\{R_1^{1/2}\}^2$. One obtains

$$\{\mathrm{VDM}\} \cong \left(4\pi a^3/\mu_0\right)\left\{(R_1/2)^{1/2}\right\}\left(1 + 5\{R_{ND}\}/4\left\{R_1^{1/2}\right\}^2\right)^{1/2}, \quad (24b)$$

or, with the numerical values obtained above, $\{\mathrm{VDM}\} \cong \{|\mathbf{m}|\}[1.1448] \cong 6.542 \times 10^{22}$ Am^2 with an uncertainty of about ±14.6%: ±11.5% in $\{|\mathbf{m}|\}$ and ±3.1% in the correction.

Table 5. Means and Standard Deviations of Reduced Paleointensity Data

Authors	Note	Quantity	Number	Time (BP)	Value ± SD, 10^{22} Am^2
McElhinny and Senanake [1982]	archeointensities	V(A)DM	14	15–50 kyr	4.44 ± 0.64
McElhinny and Senanake [1982]	10, 1 kyr means	V(A)DM	10 groups	0–10 kyr	8.75 ± 1.58
McFadden and McElhinny [1982]	their fit to a distribution	PDM	166	0–5 Myr	8.65 ± 3.6
Prévot et al. [1990, Table 1]	mean of their 12 time groups	VDM	280 in 12 groups	0–250 Myr	6.27 ± 2.95
Valet and Meynadier [1993]	initial calibration of sediment	VADM	sediment	0–4 Myr	3.9 ± 1.9
Tanaka et al. [1995]	nontransitional, T^2	VDM	340	various	8.3 ± 4.9
Juarez et al. [1998]	basaltic glass (T^2+pTRM)	VADM	21	5–160 Myr	4.2 ± 2.3
Juarez and Tauxe [2000]	T^2+pTRM and basaltic glass	VADM	70	0.3–5 Myr	5.49 ± 2.36
Selkin and Tauxe [2000]	T^2+pTRM and basaltic glass	VADM	555	0.3–300 Myr	4.6 ± 3.2
Selkin and Tauxe [2000]	T^2+pTRM and basaltic glass	VADM	2 groups	0–0.3 Myr	8.47 ± 3.10
Love and Constable [2003]	mean *F* at Hawaii and Reunion	VADM	520	0–5 Myr	8.12
Biggin and Thomas [2003]	their Group 1	V(A)DM	865	10–400 Myr	5.9 ± 3.5
Goguitchaichvili et al. [2004]	nontransitional, T^2+pTRM	VDM	902	0–5 Myr	7.69 ± 3.15
Arithmetic mean of means and RMS deviation (unweighted mean)		V(A)DM			6.52 ± 1.80
Geomagnetic estimate		{VDM}		1965–2001	6.50 ± 1.00
Geomagnetic estimate		{VADM}		1965–2001	6.51 ± 0.94

[53] A second way is to extract intensity from (23b),

$$\{\mathrm{VDM}\} \cong \left(4\pi a^3/\mu_0\right)\left\{\left(F^2/2\right)^{1/2}\left(1+R_{\mathrm{ND}}/4F^2\right)^{1/2}\right\}, \quad (25a)$$

and approximate $R_{\mathrm{ND}}/4F^2$ with $\{R_{\mathrm{ND}}\}/4\{F\}^2$. One obtains

$$\{\mathrm{VDM}\} \cong \left(4\pi a^3/\mu_0\right)(1/2)^{1/2}\{F\}\left(1+\{R_{\mathrm{ND}}\}/4\{F\}^2\right)^{1/2}, \quad (25b)$$

or, with the numerical values for $\{R_{\mathrm{ND}}\}$ and $\{F\}$ above, $\{\mathrm{VDM}\} \cong 6.447 \times 10^{22}$ Am^2. The correction to the effect of $\{F\}$ alone is 2.5%, so the uncertainty in (25c) is ±14.7%.

[54] Estimates (24b) and (25b) agree to within 1.5%, so we set $\{\mathrm{VDM}\} \cong 6.50 \times 10^{22}$ Am^2 with an uncertainty of about 15.4%. For the calibrated statistical model, $\{\mathrm{VDM}\} \cong \{\mathrm{VADM}\}$.

6. Comparisons With Mean Paleointensity Determinations

[55] The foregoing estimates for time averaged, global mean measures of magnetic field strength rely on the field determined via satellites to calibrate stationary trial probability distributions (4a) for fluctuations about expectation magnetic spectrum (3a). Estimates for RMS intensity $\{F^2\}^{1/2} = 37.3$ μT, RMS dipole field $\{R_1^c\}^{1/2} = 33.9$ μT, RMS nondipole field $\{R_{\mathrm{ND}}^c\}^{1/2} = 15.6$ μT, RMS dipole moment $\{\mathbf{m}\bullet\mathbf{m}\}^{1/2} = 6.20 \times 10^{22}$ Am^2, and absolute dipole moment $\{|\mathbf{m}|\} = 5.72 \times 10^{22}$ Am^2 use exact formulations, yet have ±11.5% uncertainties originating in the estimate of spectral amplitude. Estimates for mean intensity $\{F\} \cong 34.4 \pm 4.9$ μT, mean virtual axial dipole moment $\{\mathrm{VADM}\} \cong (6.51 \pm 0.94) \times 10^{22}$ Am^2, and mean virtual dipole moment $\{\mathrm{VDM}\} = (6.50 \pm 1.00) \times 10^{22}$ Am^2, use approximate formulations with uncertainties closer to ±15%. The estimates are about 5% greater than before, but the uncertainties are new and considerably less than typical fluctuations indicated by the dipole power variance from PD (4a). Are these estimates accurate over the geologic time intervals for which they are intended?

[56] To try to answer this question, I sought published paleomagnetic determinations of mean paleointensity. Such means differ because different authorities use different data selection criteria, different spatial distributions of data, different temporal distributions of data, and different averaging techniques. Table 5 summarizes mean values found and their standard deviations. These mean values are not statistically independent because different authorities sometimes select the same data. Such commonly selected data receive heavier weight in the simple arithmetic average of mean paleointensities shown in Table 5.

6.1. A Comparison With Archeointensity

[57] According to the archeointensity data selection and analysis of *McElhinny and Senanake* [1982], 4 VDM*s* and 10 VADM*s* from the interval 15–50 kyr BP average to $(4.44 \pm 0.64) \times 10^{22}$ Am^2. Ten, 1 kyr mean values of archeomagnetic VDM*s* (VADM*s* when necessary) for the interval 0–10 kyr BP, average to $(8.75 \pm 1.58) \times 10^{22}$ Am^2. The former is $(2.07 \pm 1.14) \times 10^{22}$ Am^2, or 32% and $1.8\sigma^*$, less than the geomagnetic estimate for {VADM}; the latter is $(2.25 \pm 1.87) \times 10^{22}$ Am^2, or 35% and $1.2\sigma^*$, greater than the estimate for {VDM}. The uncertainty in a difference, here denoted σ^*, is the root sum square of the two independent uncertainties.

[58] The two average archeointensities of *McElhinny and Senanake* [1982] differ at the $2.5\sigma^*$ level. If we accept that mean virtual moment differed significantly during these two different intervals, then we should weight the averages by interval durations, 10 kyr or 35 kyr. The resulting duration weighted mean of 5.40×10^{22} Am^2 is 17% less than the estimate for {VADM}. The twelve, 1 kyr means from 0 to 12 kyr BP tabulated by *McElhinny and Senanake* [1982] have a RMS value of 8.676×10^{22} Am^2. Their 14 select values from 17 to 50 kyr BP have a RMS value of 4.578×10^{22} Am^2. The root duration weighted mean square of the two RMS values, 5.953×10^{22} Am^2, is 16% less than the estimate for $\{\mathrm{VADM}^2\}^{1/2}$. Though seemingly insignificant in light of ±14.5% uncertainties, the geomagnetic estimates are about 17% more than these weighted mean archeointensity determinations for the past 50,000 years.

6.2. Initial Comparisons With Mean Reduced Paleointensities

[59] *McFadden and McElhinny* [1982] analyze 166 nontransitional VDM*s* for the past 5 Myr. They note reasons to

reject Gaussian, but perhaps not lognormally, distributed VDMs. Still, they find support for a model in which nondipole intensity is proportional to a "true dipole moment" that has a truncated Gaussian distribution with a standard deviation of 3.6×10^{22} Am^2 and a peak at the $(8.65 \pm 0.65) \times 10^{22}$ Am^2 "paleomagnetic dipole moment" (PDM). Curiously, their lognormal distribution peaks near 6.5×10^{22} Am^2 $\cong$ {VDM}. In contrast, PD (4a) gives a Maxwellian distribution for absolute dipole moment that requires no truncation at small moments, falls off like a Gaussian at large moments, and peaks at 5.06×10^{22} Am^2 (±11.5%).

[60] The PDM exceeds the estimated {VDM} by $(2.15 \pm 1.19) \times 10^{22}$ Am^2, or 33%. This difference amounts to a $+0.95\sigma_1$ excess in R_1^c, or 60% of the standard deviation given by *McFadden and McElhinny* [1982], but is significant at the $1.8\sigma^*$ level given the $\pm 0.65 \times 10^{22}$ Am^2 uncertainty in PDM and the $\pm 1.00 \times 10^{22}$ Am^2 uncertainty in {VDM}.

[61] *Valet and Meynadier* [1993] found a mean VADM of $(3.9 \pm 1.9) \times 10^{22}$ Am^2 from sediments formed during the past 4 Myr. This is $(2.6 \pm 2.1) \times 10^{22}$ Am^2, or 60% of and $1.2\sigma^*$ less than the estimated {VADM}. They also cite values of $(5 \pm 2) \times 10^{22}$ Am^2 for the past 140 kyr and $(4.3 \pm 1.5) \times 10^{22}$ Am^2 for the interval 15–50 kyr BP. The difference between the 5 Myr igneous PDM and the 4 Myr mean sedimentary VADM is $(4.75 \pm 2.01) \times 10^{22}$ Am^2. At $2.4\sigma^*$, this difference is more significant than the difference between either paleomagnetic determination of mean paleointensity and the geomagnetic estimate. Furthermore, it is not due to huge VDM*s* 4–5 Myr BP.

[62] Some systematic effects of calibration of relative paleointensity from sediments, sedimentation time averaging, exclusion of transitional VDM*s* from igneous rocks, and trace multidomain grains are noted in Appendix C. It was thought that some cancellation of such systematic effects results by averaging the 5 Myr PDM from volcanics [*McFadden and McElhinny*, 1982] with the 4 Myr mean VADM from sediments [*Valet and Meynadier*, 1993]. The result, 6.3×10^{22} Am^2, agrees with the estimates for {VADM} and {VDM} in section 5.

6.3. More Comparisons With Mean Reduced Paleointensities

[63] The tabulation of Cenozoic and Mesozoic Thellier-Thellier paleointensities by *Prévot et al.* [1990, Table 1] reduces 280 determinations to 12 temporal group mean VDM*s*. The unweighted mean and standard deviation of the 12 group mean VDMs is $(6.27 \pm 2.95) \times 10^{22}$ Am^2. This agrees with the estimate for {VDM} – the 3.5% difference is not significant. The weighted average, with weights equal to the square root of the number of VDM*s* in the group times the apparent duration spanned by the group, is 6.31×10^{22} Am^2. Three groups, Coniacian-Santonian, Hettangian-Sinemurian, and Early Triassic, have few samples, uncertain ages rather than definite durations, and might be over weighted. Omitting these three gives a 9 group weighted average VDM of 5.88×10^{22} Am^2. Neither weighted mean VDM differs significantly from the geomagnetic estimate for {VDM}.

[64] The *Prévot et al.* [1990] tabulation contains no data from the Cretaceous superchron (M. Prévot, personal communication, 1996). This is considered important because a purely stationary statistical model likely fails to describe both reversible and nonreversing superchron states of the core geodynamo. Indeed, *Voorhies and Conrad* [1996] describe nonstationary magnetic effects of a geologically transient, compositionally stratified, stable layer in the uppermost outer core. The effects include both suppression of reversals and the possibility that the $1/n$ modulation in expectation spectrum (3a) may give way to a diffusion dominated, n^{-3} modulation. Curiously, spectrum (3a) can be salvaged if the nonstationarity is limited to the anisotropy index defined in Appendix A. This might occur if, as seems more widely held, suppression of reversals is due mainly to anisotropy in the laterally heterogeneous heat flow across the core-mantle boundary, as simulated by *Glatzmaier et al.* [1999].

[65] *Tanaka et al.* [1995] analyzed a global paleointensity database of 1123 published volcanic flow means. Their published mean of 427 VDM*s* inferred via either Thellier or Shaw methods is $(7.4 \pm 4.9) \times 10^{22}$ Am^2. This is 0.9×10^{22} Am^2 greater than the geomagnetic estimate for {VDM}, but the difference is not significant. *Tanaka et al.* [1995] found 87, or 20.4%, of these VDM*s* to be transitional. Their published mean of nontransitional VDM*s* is $(8.3 \pm 4.9) \times 10^{22}$ Am^2, so the transitional VDM*s* average to 3.9×10^{22} Am^2, or 47% of the mean of nontransitional VDM*s*. Even using the standard error of their mean nontransitional VDM (standard deviation/$(340)^{1/2}$), their mean nontransitional VDM exceeds the estimate for {VDM} by $(1.8 \pm 1.1) \times 10^{22}$ Am^2; this difference is of dubious significance at the $1.7\sigma^*$ level.

[66] When integrated over the sphere, the model fitted by *Tanaka et al.* [1995] to nontransitional VDM*s*, $F \cong 31.3(1 + 3\cos^2 p)^{1/2}$ μT, yields $\langle F \rangle \cong 43.2$ μT. This is 26% greater than the estimate for $\{F\}$, which is itself uncertain by ±14.2%. Their model also indicates $\langle F^2 \rangle^{1/2} \cong 44.3$ μT, or 19% greater than the estimate for $\{F^2\}^{1/2}$ – still less than a $2\sigma^*$ discrepancy.

[67] *Voorhies and Conrad* [1996] analyzed the *McFadden and McElhinny* [1982] table of geographically grouped, nontransitional, flow mean VDMs and related parameters. With 48% of the samples being from Czechoslovakia or Japan, and over 48% of the samples being post-Pleiocene, the distribution is geographically and temporally nonuniform. Efforts to compensate for biases in the distribution and construct a suitable spatiotemporal average of flow mean paleointensities led to an RMS weighted intensity of 44.5 μT. This is a weighted average of group mean intensities, with each weight being the square root of the number of samples in the group multiplied by both the group mean $\sin\theta$ and the time interval apparently represented by the group. The result agrees with the value from integrating the model of *Tanaka et al.* [1995] and so remains 19% greater than expected.

6.4. Comparisons With More Recent Mean Reduced Paleointensities

[68] *Juarez et al.* [1998] present 21 paleointensity determinations from submarine basaltic glass formed at many different locations during the past 160 Myr. The mean VADM is $(4.2 \pm 2.3) \times 10^{22}$ Am^2 (L. Tauxe, personal communication, 1998). This is $(2.3 \pm 2.5) \times 10^{22}$ Am^2 less than the estimate for {VADM}. The exceptionally fine

grained, single domain magnetite carrier in such glasses need not share problems found in multidomain, and even pseudosingle domain, grains. In particular, *Xu and Dunlop* [2004] find that straight line fits through low and medium temperature points in Arai plots for small, pseudosingle domain (0.6 and 1 μm) magnetite grains overestimate the intensity of the paleofield by about 25%. Curiously, 4/3 of the estimated {VDM} is indistinguishable from the PDM.

[69] For the interval 0.3–5 Myr BP, *Juarez and Tauxe* [2000] consider both 38 existing Thellier-Thellier paleointensity determinations with pTRM checks, denoted T^2+pTRM, and 32 new values from submarine basaltic glass. Their published mean VADM for this interval, $(5.49 \pm 2.36) \times 10^{22}$ Am^2, agrees with the estimated {VADM} of $(6.51 \pm 0.94) \times 10^{22}$ Am^2.

[70] *Selkin and Tauxe* [2000] discuss data selection criteria. They select 268 of 1592 previously published absolute paleointensities and 287 paleointensities from submarine basaltic glass. Their average VADM for the combined data set is 5.4×10^{22} Am^2 with a standard deviation of $\pm 3.6 \times 10^{22}$ Am^2. The average within the 0–0.3 Ma interval is $(8.47 \pm 3.10) \times 10^{22}$ Am^2, while the average of the 0.3–300 Ma data set is $(4.6 \pm 3.2) \times 10^{22}$ Am^2. Both are listed in Table 5.

[71] *Biggin and Thomas* [2003] selected 865 of 1167 published paleointensity determinations, from which they further extract a second group of 425 and a third group of 47 based on increasingly stringent data selection criteria. The means and standard deviations of the three groups are 5.9 ± 3.5, 3.3 ± 3.1 and 5.8 ± 3.2 with units of 10^{22} Am^2. Only the first is listed in Table 5.

[72] *Love and Constable* [2003, Table 5] give the arithmetic mean and standard deviation for 457 values for paleointensity at Hawaii, 35.80 ± 12.30 μT, and for 63 values for paleointensity at Reunion, 40.29 ± 9.89 μT. Most of the data cited come from latitudes 19.5° or −21.1°, respectively, so equation (10) is used to compute 5 Myr mean VADM*s* and standard deviations from these magnetic volcanic edifices. The results are $(8.02 \pm 2.75) \times 10^{22}$ Am^2 for Hawaii and $(8.84 \pm 2.17) \times 10^{22}$ Am^2 for Reunion. If one accepts standard errors of ±0.13 and $\pm 0.27 \times 10^{22}$ Am^2 for Hawaii and Reunion, respectively, then these mean VADM*s* would seem to differ significantly, by over $2\sigma^*$. The weighted arithmetic mean of the two values, with weights equal to the number of samples, is about 8.12×10^{22} Am^2. This value is included in Table 5. It exceeds the estimate for {VADM}, $(6.51 \pm 0.94) \times 10^{22}$ Am^2, by at most $1.7\sigma^*$.

[73] *Goguitchaichvili et al.* [2004, Figure 1c] show the distribution of 902 select VDM*s* from the past 5 Myr with a mean of 7.69×10^{22} Am^2 and a standard deviation of $\pm 3.15 \times 10^{22}$ Am^2. This mean is 18% greater than the estimate for {VDM}. Even adopting a standard error for their mean of about $\pm 0.10 \times 10^{22}$ Am^2, it is only exceeds the estimate by about $1.2\sigma^*$. The truncated normal distribution plotted on their histogram Figure 1c appears to underestimate the count of VDM*s* with values less than the mean. This might be explained by contributions from an absolute dipole moment with a more nearly Maxwellian distribution.

6.5. Summary of Comparisons

[74] Table 5 summarizes 13 mean paleointensities extracted from the literature. There might be more such mean values, but this sample is enough for present purposes. The values in Table 5 prove that the range of paleomagnetically determined mean paleointensities includes the geomagnetic estimates for {VDM} and {VADM} from section 5 of about $(6.5 \pm 1.0) \times 10^{22}$ Am^2. The statistical hypothesis therefore passes the test against mean paleointensity.

[75] Though not statistically independent, the tabulated values have an arithmetic mean and RMS deviation of $(6.52 \pm 1.80) \times 10^{22}$ Am^2. This agrees very well with the geomagnetic estimate, perhaps because (1) neither duration nor the square root of the number of sample VADM*s* were used to weight this average, (2) other mean values were not found and so not included, or (3) the geomagnetic estimate is not bad.

[76] The standard deviation of each mean in Table 5 provides some indication of the width of the distribution of paleomagnetically determined VDMs and VADMs. The unsigned standard deviations average 2.76×10^{22} Am^2 with an RMS deviation of $\pm 1.05 \times 10^{22}$ Am^2. Recall that the statistical model puts the square root of the variance in core dipole power at $\sigma_1 = (2/3)^{1/2}\{R_1^c\}$. So $\pm\sigma_1$ variations in R_1^c about its mean correspond to absolute dipole moments of $[1 \pm (2/3)^{1/2}]^{1/2}$ times its expected value, or between 2.45 and 7.70×10^{22} Am^2. Half the difference between these two values, 2.62×10^{22} Am^2, is a half width describing $\pm\sigma_1$ variations in absolute dipole moment. We expect a usually mainly dipolar field, so this half width provides a rough estimate of the half width of VADM distributions compatible with the statistical model. This rough estimate agrees well with the average of the tabulated unsigned standard deviations. The agreement suggests that sample probability densities, and arguably the true PDs, are neither far more broadly nor far more sharply peaked than indicated by chi-square density (4a) for dipole power.

[77] Several studies suggest that mean paleointensity for the last 300 kyr to 5 Myr is somewhat higher than our geomagnetic estimate, perhaps by about 18% to 33% (but see *Juarez and Tauxe* [2000]). It is not clear how strongly these studies rely upon paleointensities determined at low to moderate temperatures from samples with pseudosingle domain magnetite grains as the dominant TRM carrier. This is of some concern because *Xu and Dunlop* [2004] find that straight line fits through low and medium temperature points in Arai plots for small, pseudosingle domain (0.6 and 1 μm) magnetite grains overestimate paleointensity by about 25%.

7. Summary and Conclusions

[78] A statistical hypothesis about Earth's magnetic field has been tested against paleomagnetism by combining it with the present field to estimate time averaged paleomagnetic intensity. The estimate uses the geomagnetic multipole power spectrum R_n determined from satellite era measurements. The hypothesis asserts that low-degree multipole powers of the core source field, R_n^c, are distributed as chi-square with $2n + 1$ degrees of freedom and theoretical expectation values $\{R_n^c\} = K(n + 1/2)[n(n + 1)]^{-1}(c/a)^{2n+4}$, where a is the 6371.2 km reference sphere radius and c is the 3480 km radius of Earth's core. The implied, or expectation, field on Earth's surface is usually mainly dipolar and

can be primarily axial. Amplitude K is estimated by fitting theoretical to observational spectra of degrees 1–12.

[79] The resulting calibrated expectation spectrum is summed through degree 12 to estimate expected square field intensity $\{F^2\}$. This sum also estimates mean square paleointensity, averaged over geologic time as well as the sphere, in so far as the present field spectrum is a fair sample of that generated in the past by core geodynamic processes. Previously, we excluded dominant degrees 1 and 2 from the fit, but not the sum, to predict mean paleointensity from the 1980 Magsat nondipole field. The new estimate fits all R_n of degrees 1–12 self-consistently and yields $\{F^2\} = (37.3 \pm 4.3\ \mu\text{T})^2$.

[80] Because the hypothesis requires a usually mainly dipolar field, it can be used to approximate expectation values for other measures of intensity. For example, expected paleointensity $\{F\}$ is about $34.4 \pm 4.9\ \mu$T; expected virtual axial dipole moment {VADM} is about $(6.51 \pm 0.94) \times 10^{22}$ Am^2; and expected virtual dipole moment {VDM} is about $(6.5 \pm 1.0) \times 10^{22}$ Am^2 The latter estimates are within the range of published paleomagnetic determinations of mean paleointensity; therefore the statistical hypothesis passes this test.

[81] Other statistical hypotheses about Earth's magnetic field, notably its spectrum, can clearly be tested by adaptations of the method developed and applied here. Several of these should also pass the mean paleointensity test, for the range of published mean paleointensities is fairly broad and so accommodates multipole power probability densities which differ somewhat from calibrated chi-square densities (4a). Yet the geomagnetic estimates for {VADM} and {VDM} obtained here agree well with the average of paleomagnetically determined mean values extracted from the literature. Moreover, each mean virtual moment has a standard deviation and the width of the distribution indicated by the average of unsigned standard deviations agrees with a rough estimate from the calibrated statistical model. The present model is further compatible with a field that is usually mainly that of a geocentric axial dipole. In terms of the mean square field, the dipole is also expected to be both the dominant, and the most variable, core source multipole. This can help describe the intensity and rate of dipole power excursions and, with some additional suppositions, axial dipole reversals. The statistical model offered here is thus thought to be closer to the truth than vastly different models, and so merits further development and testing.

Appendix A: Chi-Square From Nonnormal Distributions

[82] If $2n + 1$ independent variables x_i ($i = 1, 2, 3, \ldots 2n + 1$) are drawn at random from identical, zero mean Gaussian distributions of unit variance, then the probability distribution for the sum of the squares, $\Sigma_i x_i^2$, is well known to be chi-square with $2n + 1$ degrees of freedom. It is less well known that the reverse is not always true. For example, consider three independent real variables (X, Y, Z) on the open interval $(-\infty, +\infty)$ with probability densities (PDs)

$$P_{\mathrm{M}}(X) = (2\pi)^{-1/2} X^2 \exp(-X^2/2) \tag{A1a}$$

$$P_{\mathrm{D}}(Y) = \delta(Y) \tag{A1b}$$

$$P_{\mathrm{D}}(Z) = \delta(Z), \tag{A1c}$$

where P_{M} denotes the bi-Maxwellian and δ denotes the Dirac delta function. There is no chance of Y or Z being anything but zero. Because X can be either positive or negative, $P(X^2) = 2P_{\mathrm{M}}(X)|dX/d(X^2)|$. With $dX^2 = 2XdX$ and $X^2 + Y^2 + Z^2 = \chi^2$,

$$P_3(\chi^2)d\chi^2 = P(X^2)dX^2 = 2P_{\mathrm{M}}(X)|dX/d(X^2)|dX^2 \tag{A1d}$$

$$= (2\pi)^{-1/2}(X^2)^{1/2}\exp(-X^2/2)dX^2 \tag{A1e}$$

$$= \left[2^{3/2}\Gamma(3/2)\right]^{-1}(\chi^2)^{1/2}\exp(-\chi^2/2)d\chi^2 \tag{A1f}$$

where Γ is the gamma function. Distribution (A1f) is chi-square with three degrees of freedom.

[83] In example (A1), if we replace X with g_1^0/D, Y with g_1^1/D, and Z with h_1^1/D, then we describe a dipole field with no tilt and a zero mean, bimodally distributed axial component of variance $\{(g_1^0)^2\} = 3D^2$. In contrast, the isotropic case of three zero mean Gaussian distributions with equal variances for g_1^0, g_1^1 and h_1^1 describes a dipole with no preferred direction and a typical tilt of about $\tan^{-1}(2^{1/2}) = 54.7°$. This does not describe a terrestrial field dominated by a reversible axial dipole as well as example (A1), but might be of use for Uranus and Neptune. Example (A1) might be of use for Saturn [*Connerney et al.*, 1982]. Intermediate distributions seem more Earth-like and may be of use for Jupiter [*Connerney and Acuna*, 1982].

[84] There are an infinite number of sets of three probability distributions for three independent variables for which the sum of squares is distributed as chi-square with three degrees of freedom [*Voorhies and Conrad*, 1996]. Indeed, for independent variables (x_1, x_2, x_3) on $(-\infty, +\infty)$ with PDs

$$P_{\mathrm{a}}(x_1) = A_1|x_1|^{-p_1} \exp[-x_1^2/2] \tag{A2a}$$

$$P_{\mathrm{b}}(x_2) = A_2|x_2|^{-p_2} \exp[-x_2^2/2] \tag{A2b}$$

$$P_{\mathrm{c}}(x_3) = A_3|x_3|^{-p_3} \exp[-x_3^2/2] \tag{A2c}$$

and normalization constants (A_1, A_2, A_3), if the power law indices (p_1, p_2, p_3) are all less than one and sum to zero, then $x_1^2 + x_2^2 + x_3^2$ is distributed as chi-square with three degrees of freedom. There are an infinite number of such triples. The form $A|x|^{-p}\exp(-x^2/2)$ is half the chi-square distribution with typically fractional degrees of freedom $(1-p)$ reflected about zero mean; for $p = (1-2b)$, the corresponding amplitude A is $[2^b\Gamma(b)]^{-1}$. The condition $p_1 + p_2 + p_3 = 0$ implies at least one index is positive; therefore, at least one of these PDs must be singular at the origin. Such singular PDs are of dubious utility for planetary magnetism.

[85] Instead consider zero-mean Gaussian distributions for g_1^1 and h_1^1, in qualitative accord with both observations of nonzero dipole tilt and the hypothesis of zero mean tilt averaged over long geologic time intervals. Example (A1) suggests that a linear combination of Gaussian and bi-Maxwellian distributions would then yield both a regular PD for g_1^0 and a distribution for normalized dipole power $(3R_1/\{R_1\})$ equal to chi-square with three degrees of freedom.

[86] To prove this, let (x, y, z) denote scaled core dipole coefficients $[(a/c)^3g_1^0,\ (a/c)^3g_1^1,\ (a/c)^3h_1^1]$; let $(\sigma_x^2,\ \sigma_y^2,\ \sigma_z^2)$ denote the variances of these quantities; let $V^2 \equiv \sigma_x^2 + \sigma_y^2 + \sigma_z^2$; and for simplicity suppose $\sigma_y^2 = \sigma_z^2$. Now consider the probability distributions

$$P_x(x)dx = \left(3/2\pi V^2\right)^{1/2}\left(3/V^2\right)\left[\frac{\sigma_x^2-\sigma_y^2}{V^2}x^2+\sigma_y^2\right] \cdot \exp\left(-3x^2/2V^2\right)dx \tag{A3a}$$

$$P_y(y)dy = \left(2\pi\sigma_y^2\right)^{-1/2}\exp\left(-y^2/2\sigma_y^2\right)dy \tag{A3b}$$

$$P_z(z)dz = \left(2\pi\sigma_z^2\right)^{-1/2}\exp\left(-z^2/2\sigma_z^2\right)dz. \tag{A3c}$$

These are zero mean distributions, so $V^2 = (a/c)^6\{R_1^c/2\}$. For a dipole that is usually mainly axial, $\sigma_x^2 \gg \sigma_y^2$ and $P_x(x)$ is small when x^2 is small. Next define $\xi^2 \equiv x^2 + y^2 + z^2$, so $\xi^2 = (a/c)^6R_1^c/2$ and $3\xi^2/V^2 = 3R_1^c/\{R_1^c\}$. Provided (x, y, z) are statistically independent variables, it is enough to prove that $3\xi^2/V^2$ is distributed as chi-square with three degrees of freedom, or

$$P\left(\xi^2\right)d\xi^2 = \left[2^{3/2}\Gamma(3/2)\right]^{-1}\left[3\xi^2/V^2\right]^{1/2}\left[3/V^2\right] \cdot \exp\left(-3\xi^2/2V^2\right)d\xi^2 = P_3\left(\chi^2\right)d\chi^2. \tag{A3d}$$

It is also enough to prove that distribution (A3a) for an axial dipole follows from distributions (A3b), (A3c) and (A3d). This alternative is used here to show a way to derive distribution (A3a).

[87] With probability densities for the square variables denoted $Q_x(x^2)$, $Q_y(y^2)$ and $Q_z(z^2)$, the derivation begins with the fact that the distribution for ξ^2 must obey

$$P\left(\xi^2\right)d\xi^2 = \int_0^\infty\int_0^\infty\int_0^\infty Q_x\left(x^2\right)Q_y\left(y^2\right)Q_z\left(z^2\right) \cdot \left[\delta\left(\xi^2-x^2-y^2-z^2\right)\right]dx^2dy^2dz^2d\xi^2. \tag{A4a}$$

Densities (A3b) and (A3c) are symmetric, so the likelihood of y^2 is twice that of y alone and $Q_y(y^2)dy^2 = 2P_y(y)|dy/d(y^2)|dy^2 = P_y(y)|y|^{-1}dy^2$. Substitution of this relation, and a similar one for $Q_z(z^2)$, into (A4a), and making use of normal distributions (A3b) and (A3c), gives

$$P\left(\xi^2\right) = \left(2\pi\sigma_y\sigma_z\right)^{-1}\int_0^\infty\int_0^\infty\int_0^\infty Q_x\left(x^2\right) \cdot \exp\left[-y^2/2\sigma_y^2 - z^2/2\sigma_z^2\right]|yz|^{-1} \cdot \delta\left(\xi^2-x^2-y^2-z^2\right)dx^2dy^2dz^2. \tag{A4b}$$

[88] The offset delta function in (A4b) is the inverse Laplace transform, denoted L^{-1}, of the exponential of its offset,

$$\delta\left(\xi^2-x^2-y^2-z^2\right) = L^{-1}\left[\exp\left(\xi^2-x^2-y^2-z^2\right)\right] \tag{A5a}$$

$$= (2\pi i)^{-1}\int_{-i\infty}^{+i\infty}\exp\left(s\xi^2\right)\exp\left[-s\left(x^2+y^2+z^2\right)\right]ds, \tag{A5b}$$

where s denotes the Laplace transform domain variable and $i^2 = -1$ (see, e.g., *Reif* [1965, equation A.7.14] with his Fourier $k = -is$). With definitions $u \equiv x^2$, $v \equiv y^2$ and $w \equiv z^2$, substitution of (A5b) into (A4b) and a reordering of the integrations yields

$$P\left(\xi^2\right) = \left(4\pi^2 i\sigma_y\sigma_z\right)^{-1}\int_{-i\infty}^{i\infty}\int_0^\infty\int_0^\infty\int_0^\infty Q_x(u) \cdot \exp\left(s\xi^2 - su\right)\exp\left(-sv - v/2\sigma_y^2\right) \times \exp\left(-sw - w/2\sigma_z^2\right)(vw)^{-1/2}dudvdwds. \tag{A6a}$$

[89] In equation (A6a), the integrals over u, v and w are themselves Laplace transforms, so

$$P\left(\xi^2\right) = \left(4\pi^2\sigma_y\sigma_z i\right)^{-1}\int_{-i\infty}^{i\infty} L[Q_x(u)]L\left[v^{-1/2}\exp\left(-v/2\sigma_y^2\right)\right] \cdot L\left[w^{-1/2}\exp\left(-w/2\sigma_z^2\right)\right]\exp\left(s\xi^2\right)ds. \tag{A6b}$$

The transform $L[t^{q-1}e^{\alpha t}] = \Gamma(q-1)[s-\alpha]^{-q}$ for $q > 0$ is helpful [see, e.g., *Beyer*, 1978]. Indeed, because $L[w^{-1/2}\exp(-w^2/2\sigma_z^2)] = \Gamma(1/2)[(s + 1/2\sigma_z^2)]^{-1/2}$, equation (A6b) is just

$$P\left(\xi^2\right) = \left(4\pi^2\sigma_y\sigma_z i\right)^{-1}\int_{-i\infty}^{i\infty} L[Q_x(u)][\Gamma(1/2)]^2 \cdot \left[\left(s+1/2\sigma_y^2\right)\left(s+1/2\sigma_z^2\right)\right]^{-1/2}\exp\left(s\xi^2\right)ds. \tag{A6c}$$

The Laplace transform of (A6c) with respect to ξ^2 is

$$L\left[P\left(\xi^2\right)\right] = \left(2\pi\sigma_y\sigma_z\right)^{-1}L[Q_x(u)][\Gamma(1/2)]^2 \cdot \left[\left(s+1/2\sigma_y^2\right)\left(s+1/2\sigma_z^2\right)\right]^{-1/2}. \tag{A6d}$$

[90] With $\sigma_y^2 = \sigma_z^2$, the transform of (A3d) is

$$L\left[P\left(\xi^2\right)\right] = \left[2^{3/2}\right]^{-1}\left[3/V^2\right]^{1/2}\left[3/V^2\right] \cdot \left(s + 3/2V^2\right)^{-3/2}. \quad \text{(A7)}$$

This is substituted into (A6d) and the result solved for

$$L[Q_x(u)] = \sigma_y^2\left[3/2V^2\right]^{1/2}\left[3/V^2\right]\left(s + 1/2\sigma_y^2\right) \cdot \left(s + 3/2V^2\right)^{-3/2}. \quad \text{(A8)}$$

[91] The inverse transform of (A8), which gives $Q_x(u \equiv x^2)$ and thus the density $P_x(x)$ we seek, has two contributions:

$$L^{-1}\left[\left(s + 3/2V^2\right)^{-3/2}\right] = [\Gamma(3/2)]^{-1}u^{1/2}\exp\left(-3u/2V^2\right) \quad \text{(A9a)}$$

$$L^{-1}\left[s\left(s + 3/2V^2\right)^{-3/2}\right] = \pi^{-1/2}\left[u^{-1/2} - 2\left(3/2V^2\right)u^{1/2}\right] \cdot \exp\left(-3u/2V^2\right). \quad \text{(A9b)}$$

We substitute these expressions into the inverse Laplace transform of (A8), note $\Gamma(3/2) = \pi^{1/2}/2$, and multiply by dx^2 to obtain

$$Q_x\left(x^2\right)dx^2 = \sigma_y^2\left[3/2V^2\right]^{1/2}\left(2/\pi^{1/2}\right)\left[3/V^2\right] \cdot \left[\left(1/2\sigma_y^2\right)\left(x^2\right)^{1/2} + \left(x^2\right)^{-1/2}/2 - \left(3/2V^2\right)\left(x^2\right)^{1/2}\right] \cdot \exp\left(-3x^2/2V^2\right)dx^2. \quad \text{(A10)}$$

With distribution (A10), because $Q_x(x^2)dx^2 = 2P_x(x)|dx/d(x^2)|dx^2 = P_x(x)|x|^{-1}dx^2$,

$$P_x(x)dx^2 = \left[3/2\pi V^2\right]^{1/2}\left[3/V^2\right] \cdot \left[\sigma_y^2 + \left(1 - 3\sigma_y^2/V^2\right)x^2\right] \cdot \exp\left(-3x^2/2V^2\right)dx^2 \quad \text{(A11a)}$$

$$P_x(x)dx = \left(3/2\pi V^2\right)^{1/2}\left(3/V^2\right)\left[\frac{\sigma_x^2 - \sigma_y^2}{V^2}x^2 + \sigma_y^2\right] \cdot \exp\left(-3x^2/2V^2\right)dx \quad \text{(A11b)}$$

This is distribution (A3a), a linear combination of zero mean bi-Maxwellian and zero mean Gaussian distributions (QED).

[92] Note that $\sigma_x^2 - \sigma_y^2 = V^2 - 3\sigma_y^2 > 0$. For typically small tilt, $\sigma_x^2 \gg \sigma_y^2$ and the zero mean symmetric distribution (A3a) has two peaks on either side of the local minimum at $x = 0$ (or $g_1^0 = 0$ as x is $(a/c)^3 g_1^0$). The two peaks correspond to two axial dipole polarities, one normal, the other reversed. An index of anisotropy, or tilt control parameter, for distributions (A3a), (A3b), and (A3c) is $\varepsilon^* = [\sigma_x^2 - \sigma_y^2]/V^2$; this is 1 for purely axial dipoles, zero for randomly oriented dipoles drawn from an isotropic distribution, and $-1/2$ for purely equatorial dipoles. For purely axial dipoles with $\sigma_y^2 = \sigma_z^2 = 0$, distribution (A3a) would vanish at $x = 0$, hence $g_1^0 = 0$. The probability of g_1^0 passing through zero would then be zero, so reversals would be prohibited. More generally, inhibition of reversals can be described by values of ε^* very close to unity. This is inseparable from typically small tilt due to the limited descriptive power of distributions (A3a)–(A3d).

[93] It is conjectured that distributions (A3a), (A3b), and (A3c) with $0 < \varepsilon^* < 1$ describe the terrestrial dipole with fair accuracy. Very slow change of the variances (σ_x^2, $\sigma_y^2 \approx \sigma_z^2$) over very long geologic times may describe some effects of very slow changes in boundary conditions on the outer core. These distributions might also be used to help describe other planetary dipoles (e.g., ε^* seems to be near 1 for Saturn, somewhat less than one for Jupiter, and near zero for Uranus and Neptune). Of course, these distributions are but one class of core dipole coefficient distributions that are consistent with the normalized core source dipole power being distributed as chi-square with three degrees of freedom.

Appendix B: Lognormal Versus Chi-Square Distributions

[94] To show that a chi-square distribution near its mean is more closely approximated by a lognormal than a Gaussian distribution, first define $z_n \equiv R_n/\{R_n\} = \chi^2/(2n + 1)$. Then use probability densities (4a) or (4b) to rewrite distributions (4c) as

$$P_{2n+1}\left(\chi^2\right)d\chi^2 = \left[2^{n+1/2}\Gamma\left(n + {}^1\!/\!_2\right)\right]^{-1}[(2n+1)z_n]^{n-1/2} \cdot \exp[-(2n+1)z_n/2](2n+1)dz_n. \quad \text{(B1)}$$

Whereas $[z_n]^{n-1/2} = \exp[(n - {}^1\!/\!_2)\ln z_n]$,

$$P_{2n+1}\left(\chi^2\right)d\chi^2 = \left[\Gamma\left(n + {}^1\!/\!_2\right)\right]^{-1}\left(n + {}^1\!/\!_2\right)^{n+1/2} \cdot \exp\left[\left(n + {}^1\!/\!_2\right)(\ln z_n - z_n) - \ln z_n\right]dz_n. \quad \text{(B2)}$$

[95] The series expansion for the gamma function [*Gradshteyn and Ryzhzik*, 1980] is

$$\Gamma\left(n + {}^1\!/\!_2\right) = \left[2\pi/\left(n + {}^1\!/\!_2\right)\right]^{1/2}\left(n + {}^1\!/\!_2\right)^{(n+1/2)} \cdot \exp\left[-\left(n + {}^1\!/\!_2\right)\right] \times \left[1 + 12/\left(n + {}^1\!/\!_2\right) + 1/288\left(n + {}^1\!/\!_2\right)^2 + \ldots\right]. \quad \text{(B3)}$$

The first term alone approximates Γ with errors less than 5.8% for $n \geq 1$. We substitute this approximation into distributions (B2) to obtain

$$P_{2n+1}\left(\chi^2\right)d\chi^2 \cong \left[\left(n + {}^1\!/\!_2\right)/2\pi\right]^{1/2}(1/z_n) \cdot \exp\left[\left(n + {}^1\!/\!_2\right)(1 + \ln z_n - z_n)\right]dz_n. \quad \text{(B4)}$$

[96] The mean of a chi-square distribution is at $\chi^2 = 2n + 1$, or $z_n = 1$. Near the mean, $z_n \cong 1$ and, specifically for $0 < z_n \leq 2$,

$$\ln z_n = (z_n - 1) - (z_n - 1)^2/2 + (z_n - 1)^3/3 - \ldots \quad \text{(B5)}$$

When this identity is substituted into the argument of the exponential in approximation (B4), terms of first order in $(z_n - 1)$ cancel. To retain only the second-order term would give

$$P_{2n+1}\left(\chi^2 \cong 2n+1\right) d\chi^2 \approx \left[\left(n + {}^1\!/\!_2\right)/2\pi\right]^{1/2} \cdot (1/z_n) \exp\left[-\left(n + {}^1\!/\!_2\right)(z_n - 1)^2/2\right] dz_n. \quad \text{(B6)}$$

This is $1/z_n$ times a unit mean Gaussian in z_n with variance $1/(n + {}^1\!/\!_2)$.

[97] For $z_n \cong 1$, however, the argument of the exponential in (B4),

$$\left(n + {}^1\!/\!_2\right)[1 + \ln z_n - z_n] = -\left(n + {}^1\!/\!_2\right) \cdot \left[(z_n - 1)^2/2 - (z_n - 1)^3/3 + (z_n - 1)^4/4 - \ldots\right], \quad \text{(B7a)}$$

is more closely approximated by

$$-\left(n + {}^1\!/\!_2\right)(\ln z_n)^2/2 \cong -\left(n + {}^1\!/\!_2\right) \cdot \left[(z_n - 1)^2/2 - (z_n - 1)^3/2 + 11(z_n - 1)^4/24 - \ldots\right] \quad \text{(B7b)}$$

than by $-(n + {}^1\!/\!_2)[(z_n - 1)^2/2]$ alone; therefore a more accurate approximation than (B6) is

$$P_{2n+1}\left(\chi^2 \cong 2n+1\right) d\chi^2 \cong \left[\left(n + {}^1\!/\!_2\right)/2\pi\right]^{1/2} (1/z_n) \cdot \exp\left[-\left(n + {}^1\!/\!_2\right)(\ln z_n)^2/2\right] dz_n. \quad \text{(B8)}$$

This closer approximation is $1/z_n$ times a zero mean normal in $\ln z_n$, or lognormal in z_n, with variance $1/(n + {}^1\!/\!_2)$ in $\ln z_n$. A chi-square distribution near its mean is therefore more closely approximated by a lognormal than by the Gaussian distribution (QED). To order $(z_n - 1)^3$, the error reduction amounts to a factor of 2 in the exponent.

[98] Use of either lognormal or Gaussian distributions of residuals to estimate an expectation spectrum by least squares omits the factor of $1/z_n$ in either (B8) or (B6), respectively. Curiously, this should help recover the mean, as distinct from the most likely, value of χ^2.

Appendix C: Systematic Effects in Sedimentary VADMs and Volcanic VADMs

[99] A different calibration of relative paleointensity from sediments against Thellier-Thellier paleointensi ties from igneous rocks could increase the 4 Myr mean VADM from sediments [*Valet and Meynadier*, 1993; *Meynadier et al.*, 1994]. Similarly, exclusion of some Shaw data could reduced the 5 Myr mean PDM of *McFadden and McElhinny* [1982]. However, different is not necessarily better and it is not entirely clear what sort of data recalibration and/or reselection would vastly improve the accuracy of a mean paleointensity determination.

[100] It is clear that a single sedimentary sample intensity of the mean vector field averaged over sample formation time Δt, $|\int \mathbf{B} dt|/\Delta t$, can underestimate time averaged intensity, $\int |\mathbf{B}| dt/\Delta t$. This is because an oscillating field perpendicular to the mean field contributes positively to time averaged intensity $\int |\mathbf{B}| dt/\Delta t$, but tends to cancel out of the intensity of the time average vector $|\int \mathbf{B} dt|/\Delta t$. An integral number of oscillations per sample formation, or sedimentary acquisition, time cannot be generally assumed; however, appreciable cancellation is expected for periods short compared with the acquisition time. For acquisition times of order 10^2 years or less, the arguably small bias seems a small price to pay for the dense and uniform temporal distribution of sedimentary samples relative to volcanic samples.

[101] An average of nontransitional VDM*s* from volcanics can overestimate time averaged VDM simply because transitional VDM*s* are typically less than nontransitional VDM*s*, apparently by a factor of 2 (see section 6.3). Yet there are reasons to think that the many studies of axial dipole reversals have led to a relative oversampling of transitional VDM*s*. The latter can be omitted from a paleomagnetic determination of mean VDM to avoid a more serious underestimate. Of greater concern here is systematic overestimation of paleointensity resulting from omission of small but important curvature in NRM-pTRM curves caused by trace concentrations of multidomain grains [*Xu and Dunlop*, 1995, 2004]. A large curvature is more easily seen and is often used to help identify a sample as unsuitable for inclusion in a reliable absolute paleointensity determination from igneous rocks.

[102] **Acknowledgments.** Special thanks to T. Sabaka for coefficients, graphics, and helpful comments, to H. Frey for sound advice, and to J. LaBrecque. My thanks to the people of the USA who supported this work via NASA Research and Technical Operation Plans 579-31-07, 579-31-07-08, 622-72-03, and 622-70-55.

References

Benton, E. R. (1992), Hydromagnetic scale analysis at Earth's core-mantle boundary, *Geophys. Astrophys. Fluid Dyn.*, *67*, 259–272.

Beyer, W. H. (1978), *Standard Mathematical Tables*, 25th ed., 613 pp., CRC Press, Boca Raton, Fla.

Biggin, A. J., and D. N. Thomas (2003), Analysis of long-term variations in the geomagnetic poloidal field intensity and evaluation of their relationship with global geodynamics, *Geophys. J. Int.*, *152*, 392–415.

Cain, J. C., B. Holter, and D. Sandee (1990), Numerical experiments in geomagnetic modeling, *J. Geomagn. Geoelectr.*, *42*, 973–987.

Connerney, J. E. P., and M. Acuna (1982), Jovimagnetic secular variation, *Nature*, *297*, 313–315.

Connerney, J. E. P., N. Ness, and M. Acuna (1982), Zonal harmonic model of Saturn's magnetic field from Voyager 1 and 2 observations, *Nature*, *298*, 44–46.

Constable, C. G., and R. L. Parker (1988), Statistics of the geomagnetic secular variation for the past 5 Myr, *J. Geophys. Res.*, *93*, 11,569–11,581.

Constable, C. G., L. Tauxe, and R. L. Parker (1998), Analysis of 11 Myr of geomagnetic intensity variation, *J. Geophys. Res.*, *103*, 17,735–17,748.

Glatzmaier, G. A., R. S. Coe, L. Hongre, and P. H. Roberts (1999), The role of the Earth's mantle in controlling the frequency of geomagnetic reversals, *Nature*, *401*, 885–890.

Goguitchaichvili, A., J. Urrutia-Fucugauchi, L. M. Alva-Valdivia, J. Moreales, J. Riisager, and P. Riisager (2004), Long-term variation of geomagnetic field strength: A cautionary note, *Eos Trans. AGU*, *85*, 209.

Gradshteyn, I. S., and I. M. Ryzhzik (1980), *Table of Integrals, Series, and Products*, edited by A. Jeffrey, 1160 pp., Elsevier, New York.

Hulot, G., and J.-L. LeMouël (1994), A statistical approach to the Earth's main magnetic field, *Geophys. J. Int.*, *108*, 224–246.
Jacobs, J. A. (1994), *Reversals of the Earth's Magnetic Field*, 346 pp., Cambridge Univ. Press, New York.
Juarez, M. T., and L. Tauxe (2000), The intensity of the time averaged geomagnetic field: The last 5 Myr, *Earth Planet. Sci. Lett.*, *175*, 169–180.
Juarez, M., L. Tauxe, J. S. Gee, and T. Pick (1998), The intensity of the Earth's magnetic field over the past 160 million years, *Nature*, *394*, 878–880.
Langel, R. A. (1987), The main field, in *Geomagnetism*, vol. 1, edited by J. A. Jacobs, pp. 249–512, Elsevier, New York.
Langel, R. A., and R. H. Estes (1982), A geomagnetic field spectrum, *Geophys. Res. Lett.*, *9*, 250–253.
Langel, R. A., and R. H. Estes (1985), The near-Earth magnetic field at 1980 determined from Magsat data, *J. Geophys. Res.*, *90*, 2495–2509.
Love, J. J., and C. G. Constable (2003), Gaussian statistics for palaeomagnetic vectors, *Geophys. J. Int.*, *152*, 515–565.
McElhinny, M. W., and W. E. Senanake (1982), Variations in the geomagnetic dipole 1: The past 50,000 years, *J. Geomagn. Geoelectr.*, *34*, 39–51.
McFadden, P. L., and M. W. McElhinny (1982), Variations in the geomagnetic dipole 2: Statistical analysis of VDMs for the past 5 million years, *J. Geomagn. Geoelectr.*, *34*, 163–189.
McLeod, M. G. (1985), Statistical theory of the geomagnetic field and its secular variation, *Eos Trans. AGU*, *66*(46), 878.
McLeod, M. G. (1996), Spatial and temporal power spectra of the geomagnetic field, *J. Geophys. Res.*, *101*, 2745–2763.
Merrill, R. T., and M. W. McElhinny (1983), *The Earth's Magnetic Field*, 401 pp., Elsevier, New York.
Meynadier, L., J.-P. Valet, F. C. Bassinot, N. J. Shackelton, and Y. Guyodo (1994), Asymmetrical saw-tooth pattern of the geomagnetic field intensity from equatorial sediments in the Pacific and Indian oceans, *Earth Planet. Sci. Lett.*, *126*, 109–127.
Prévot, M., E. M Derder, M. McWilliams, and J. Thompson (1990), Intensity of Earth's magnetic field: Evidence for a Mesozoic dipole low, *Earth Planet. Sci. Lett.*, *97*, 1129–1139.
Reif, F. (1965), *Fundamentals of Statistical and Thermal Physics*, 649 pp., McGraw-Hill, New York.
Sabaka, T. J., N. Olsen, and R. A. Langel (2002), A comprehensive model of the quiet time, near-Earth magnetic field: Phase 3, *Geophys. J. Int.*, *151*, 32–68.
Sabaka, T. J., N. Olsen, and M. E. Purucker (2004), Extending comprehensive models of the Earth's magnetic field with Oersted and CHAMP data, *Geophys. J. Int.*, *159*, 521–547, doi:10.1111/j.1365-246X.2004.02421.x.
Selkin, P. A., and L. Tauxe (2000), Long-term variations in palaeointensity, *Philos. Trans. R. Soc. London, Ser. A*, *358*, 1065–1088.
Stevenson, D. J. (1983), Planetary magnetic fields, *Rep. Prog. Phys.*, *46*, 555–620.
Valet, J.-P., and L. Meynadier (1993), Geomagnetic field intensity and reversals during the past four million years, *Nature*, *366*, 234–237.
Voorhies, C. V. (2004), Narrow-scale flow and a weak field by the top of Earth's core: Evidence from Ørsted, Magsat and secular variation, *J. Geophys. Res.*, *109*, B03106, doi:10.1029/2003JB002833. (Correction, *J. Geophys. Res.*, *109*, B08103, doi:10.1029/2994JB003289.)
Voorhies, C. V., and J. Conrad (1996), Accurate predictions of mean geomagnetic dipole excursion and reversal frequencies, mean paleomagnetic intensity, and the radius of Earth's core using McLeod's rule, *NASA Tech. Memo.*, *TM-104634*, 35 pp.
Voorhies, C. V., T. J. Sabaka, and M. Purucker (2002), On magnetic spectra of Earth and Mars, *J. Geophys. Res.*, *107*(E6), 5034, doi:10.1029/2001JE001534.
Tanaka, H. M., M. Kono, and H. Uchimura (1995), Some global features of paleointensity in geological time, *Geophys. J. Int.*, *120*, 97–102.
Xu, S., and D. J. Dunlop (1995), Thellier paleointensity determination using PSD and MD grains, *Eos Trans. AGU*, *76*(46), Fall Meet. Suppl, F170.
Xu, S., and D. J. Dunlop (2004), Thellier paleointensity theory and experiments for multidomain grains, *J. Geophys. Res.*, *109*, B07103, doi:10.1029/2004JB003024.

C. V. Voorhies, Planetary Geodynamics, Code 698, NASA Goddard Space Flight Center, Greenbelt, MD 20771, USA. (coerte.v.voorhies@nasa.gov)